University of Stavanger

Faculty of Science and Technology

MASTER'S THESIS

Study program/ Specialization: **Petroleum Engineering/** **Reservoir Engineering**	Spring semester, 2011.... Open / Restricted access
Writer: **Hojatollah Moradi**	…… (Writer's signature)

Faculty supervisor: **Dr. Dimitrios G. Hatzignatiou**

External supervisor(s): **Arne Stavland**

Titel of thesis:

Experimental investigation of polymer flow through water- and oil-wet porous media

Credits (ECTS): **30**

Key words:	Pages: 67 + enclosure: 2 CD Stavanger, July 2011 Date/year

Abstract

The majority of the research conducted on polymer behavior in porous media is either for single phase flow or water-wet cores. The effect of wettability on polymer behavior in porous media is the main focus of this work.

In the first part of this study, the bulk rheology of two hydrolyzed polyacrylamides (HPAM), with different molecular weight, dissolved in two brines with different salinities has been studied. A Carreau-type model was fitted on all measured data and the effect of salinity and molecular weight on the rheological properties of these two HPAMwas investigated.

For the core flooding experiments, a new setup was implemented in which, instead of measuring manually the core effluent concentrations during the polymer flooding, a capillary tube was connected to the core outlet. Using the notion of the intrinsic viscosity, a formula was derived to estimate the polymer concentration from the pressure drop recorded across the capillary tube. In addition, basic properties related to polymer flow in porous media, such as polymer adsorption, inaccessible pore volume, LIST ANY OTHER RELEVANT PROPERTIES HERE, were evaluated for all four cores and wetting conditions.

In order to find out polymer behavior under different wettability conditions, it is very favorable to conduct the experiments on cores with various wettabilities but the same pore structure. Therefore two Berea and two Bentheim cores were selected with the wettability of one core from each type been altered to oil-wet.

A series of polymer and water floodings were performed during which the polymer properties in porous media were calculated and the cores' wettability evaluated based on the measured laboratory data.

From the experiments mentioned above, several important finding are reported. All polymer solutions showed both upper Newtonian and shear thinning flow regimes in our bulk rheology investigation. The effect of brine salinity on polymer viscosities was significant. From the core flooding experiments, both polymer shear thickening and degradation flow regimes on the two water-wet cores were observed. The Berea water-wet core had the highest value of retention and IPV. Lowest retention was also observed in the Berea oil-wet, which means that the core wettability had a significant effect on polymer behavior in porous media.

ACKNOWLEDGEMENT

This dissertation would not have been possible without the guidance and the help of several individuals who in one way or another contributed and extended their valuable assistance in the preparation and completion of this study.

I am heartily thankful to my supervisors, Dr. Dimitrios Georgios Hatzignatiou and Arne Stavland, whose encouragement, guidance and support from the initial to the final level enabled me to develop an understanding of the subject. I also appreciate the support I got from all my colleagues in IRIS.

At the end, I am grateful to my family who supported me in every respect during the completion of this project.

Hojatollah Moradi

List of the tables

Table 3.1 Polymer properties.

Table 3.2 Brine compositions and salinities.

Table 3.3 Core samples properties.

Table 4.1 Parameters used to match the polymer 3630 in SSW viscosity to a Carreau model

Table 4.2 Parameters used to match the polymer 3630 in NF-SW viscosity with a Carreau model

Table 4.3 Parameters used to match the polymer 3230 in SSW viscosity to a Carreau model

Table 4.4 Parameters used to match the polymer 3230 in NF-SW viscosity to a Carreau model

Table 4.5 Parameters used to match the 400 ppm polymer 3630 in SSW viscosity to a Carreau model

Table 4.6 Intrinsic viscosity and Huggins constant

Table 5.1 Apparent viscosity from Darcy law in second polymer flooding

Table 5.2 Multi rate polymer flooding parameters

Table 5.3 Summary of results, water-wet core samples

Table 6.1 Apparent viscosity from Darcy law in second polymer flooding

Table 6.2 Oil-wet cores parameters

Table A.1 Measured viscosity using the polymer 3630 in SSW at 20°C.

Table A.2 Measured viscosity using the polymer 3630 in NF at 20°C.

Figure A.3 Measured and matched viscosity versus shear rate, 3230S in SSW

Figure A.4 Measured and matched viscosity versus shear rate, 3230S in NF

List of figures

Figure 2.1 Viscosity versus shear rate of xanthan solution at a range of polymer concentration (after Chauveteau, 1982)

Figure 2.2 Comparision of power law model and Careau model, (after Sobbie, 1991)

Figure 2.3 Schematic diagram of polymer retention mechanisms in porous media (after Sorbie, 1991)

Figure 3.1 Anton Paar MCR 301 rheometer (from www.anton-paar.com)

Figure 4.1 Measured and matched viscosity versus shear rate, 3630 in SSW

Figure 4.2 Measured and matched viscosity versus shear rate, 3630 in NF-SW

Figure 4.3 Measured and matched viscosity versus shear rate, 3230 in SSW

Figure 4.4 Measured and matched viscosity versus shear rate, 3230 in NF-SW

Figure 4.5 Measured and matched viscosity versus shear rate, 400 ppm 3630 in SSW

Figure 4.6 Derived Intrinsic viscosity and Huggins constant for the 3630S in SSW

Figure 4.7 Calculated effective viscosity of SSW and 400 ppm 3630 in SSW solution in various shear rates from capillary tube flooding

Figure 4.8 Calculated effective viscosity of SSW and 400 ppm 3630 in SSW solution in various injection rates from capillary tube flooding

Figure 4.9 Huggins constant corresponding to shear rate of 130 s-1 for the 3630S in SSW

Figure 4.10 Calculated pressure drops over capillary tube versus normalized concentration of polymer solution

Figure 5.1 Pressure profile of SSW injection in 0.2 ml/min through Bentheim water-wet

Figure 5.2 Oil recovery from SSW injection of 0.2 ml/min through Bentheim water-wet core

5.3 Polymer breakthrough in the first polymer flooding through Bentheim water-wet core

5.4 Polymer breakthrough in second polymer flooding through Bentheim water-wet core

5.5 Water breakthrough in water flooding after first polymer flooding through Bentheim water-wet core

Figure 5.6 Multi rate Polymer flooding through Bentheim water-wet core

Figure 5.7 Darcy apparent viscosity and Carreau model for bulk viscosity, Bentheim water-wet core

Figure 5.8 Resistance factor and apparent viscosity

Figure 5.9 Oil recovery of SSW injection in 0.9 ml/min through Berea water-wet core

Figure 5.10 Pressure profile of SSW injection in 0.9 ml/min through Berea water-wet

Figure 5.11 Water production, Brea water-wet

Figure 5.12 Pressure profile of oil injection in the rate of 2 ml/min through Berea water-wet

5.13 Polymer breakthrough in the first polymer flooding through Berea water-wet core

5.14 Polymer breakthrough in the second polymer flooding through Berea water-wet core

Figure 5.15 Multi rate Polymer flooding

Figure 5.16 Calculated apparent viscosity in the core versus polymer injection rate

Figure 5.16 Effective viscosities of injection polymer solution and effluent fluid in Capillary tube, Berea water-wet core

Figure 5.17 Resistance factor and apparent viscosity, Berea water-wet core

Figure 6.1 Pressure profile of SSW injection in 0.9 ml/min through Bentheim oil-wet

Figure 6.2 Pressure drop across the core during water flooding, Bentheim oil-wet

Figure 6.3 Polymer breakthrough in the first polymer flooding through Bentheim oil-wet core

6.4 Polymer breakthrough in second polymer flooding through Bentheim water-wet core

Figure 6.5 Water breakthrough in water flooding after first polymer flooding through Bentheim oil-wet core

Figure 6.6 Multi rate Polymer flooding through Bentheim water-wet core

Figure 6.7 Darcy apparent viscosity, Bentheim oil-wet core

Figure 6.9 Oil recovery of SSW injection in 0.9 ml/min through Berea oil-wet core

Figure 6.10 Pressure profile of SSW injection in 0.9 ml/min through Berea oil-wet

Figure 6.11 Polymer breakthrough in the first polymer flooding through Berea oil-wet core

Figure 6.12 Polymer breakthrough in the second polymer flooding through Berea oil-wet core

Figure 6.13 Water breakthrough in water flooding after first polymer flooding through Berea oil-wet core

Figure 6.14 Multi rate Polymer flooding through Berea oil-wet core

Figure 6.15 Multi rate water flooding through Berea oil-wet core

Figure 6.16 Third polymer flooding through Berea oil-wet core

Figure 7.1 Effect of solvent salinity on viscosity of polymer 3630

Figure 7.1 Effect of solvent salinity on viscosity of polymer 3630

Figure 7.3 Effect of polymer molecular weight

Figure 7.4 Normalized oil recovery, Berea cores

Figure 7.5 Normalized oil recovery, Berea cores (1st pore volume injected)

Figure 7.6 Normalized oil recovery, Bentheim cores

Figure 7.7 Normalized oil recovery, Bentheim cores (1st Pore volume injected)

Figure 7.8 Breakthrough time in first polymer flooding for both Bentheim and Berea water-wet cores

Figure 7.9 Breakthrough times in first and second polymer flooding for Berea oil-wet cores

Figure 7.10 Breakthrough time in first polymer flooding for both Berea oil-wet and water-wet cores

Contents

Abstract **2**
1. Introduction **10**
2. Theory 12
2.1. Introduction 12
2.2. Property and bulk rheology of synthetic polymer 12
2.2.1. Molecular weight and intrinsic viscosity 12
2.2.2. Bulk rheology 13
2.3. Newtonian and non-Newtonian fluid flow through capillary tube 15
2.3.1. Newtonian fluid 15
2.3.2. Non-Newtonian fluid 15
2.4. Polymer flow through porous media 16
2.4.1. Polymer retention in porous media 16
2.4.2. Polymer rheology in porous media 17
3. Experiments **19**
3.1. Chemicals 19
3.2. Bulk viscosity measurements 20
3.3. Core flooding Experiments 20
3.4. Core flooding Procedure 21
4. Polymer Rheology **23**
4.1. Introduction 23
4.2. Bulk viscosity versus shear rate 23
4.3. Intrinsic viscosity 25
4.4. Polymer flow through capillary tube 29
5. Polymer Flow in water-wet core samples **32**
5.1. Introduction 32
5.2. Bentheim water-wet Core sample 32
5.2.1. Wettability 32
5.2.2. Polymer effects on porous media 33
5.2.3. Apparent viscosity and resistance factor 36
5.3. Berea water-wet Core sample 39
5.3.1. Wettability 39
5.3.2. Polymer effects on porous media 41
5.3.3. Apparent viscosity and resistance factor 43
5.4. Summary 46
6. Polymer Flow in oil-wet core samples **47**
6.1. Introduction 47
6.2. Bentheim oil-wet Core sample 47

6.2.1. Wettability 47
6.2.2. Polymer effects on porous media 48
6.2.3. Apparent viscosity and resistance factor 45
6.3. Berea oil-wet Core sample 51
6.3.1. Wettability 51
6.3.2. Polymer effects on porous media 52
6.4. Summary 56
7. Discussion and conclusion **57**
8. Conclusion and recommendation

Appendix **64**
Refferences **67**

1 Introduction

In order to maintain reservoir pressure and also to sweep out oil efficiently, water flooding became the standard practice in many reservoir formations. The efficiency of the water flood oil displacement mechanism as a result of an unfavorable mobility ratio identified.

Macroscopic displacement efficiency is then improved by maintenance of favorable mobility ratios between oil and water through reservoirs. Polymer solutions are designed to develop a favorable mobility ratio between injected polymer solution and the oil or water bank being displaced a head of the polymer. The purpose is to develop a more uniform volumetric sweep of the reservoir, both vertically and aerially.

The mobility ratio defines as:

$$M = \frac{(\mu_o / k_0)}{(\mu_w / k_w)}$$

Where μ and k are viscosity and effective permeability respectively and subscribe o and w refer to oil and water. In order to mobilize the residual oil it is necessary to increase the viscous to capillary force balance between the water and oil phases in the displacement.

Polymers could significantly increase the injected brine viscosity by factor of 3 to 20 with very low concentration.

Since polymer behavior in porous media from bulk behavior, Lots of works has been done on describing polymer rheology behavior. Most of the works has been performed on water wet porous media due to the complexity of polymer behavior and majority of studies are in single phase flow.

In this work, polymer rheology in porous media in presence of oil will present effect of wettability on parameters related to polymer flooding will investigated.In order to have good comparison between polymer behavior in oil-wet and water-wet porous media, two types of core samples which their wettability had been altered were used and result has been presented.

The sequence of presentation is as follows:

In chapter 2, chemical and their properties are presented, as well as, cores properties and core flooding procedure.

In chapter 3, Bulk rheology of synthetic polymers is discussed and Careau model are matched to measured data. Non-Newtonian fluid flow in capillary tube is investigated and

simple model to predict the pressure in capillary tube which flooded with various concentration of polymer, were derived.

The majority of work which is core flooding is discussed in chapter 4 for water-wet cores and chapter 5 for oil-wet ones. The result and interpretation of polymer flooding parameters are presented in these chapters.

At the end the result for oil-wet and water-wet cores are compared in chapter 7.

2 Theory

2.1 Introduction

Polymers are added to brine in waterflood in order to increase the viscosity of the injection fluid to improve the mobility ratio between oil and water.

The two most commonly used polymers in EOR processes are the synthetic polymers and bio polymers. One good example for synthetic polymers is hydrolyzed polyacrylamide, in its partially hydrolyzed form, HPAM and example for biopolymers is xanthan.

HPAM has been used in oil recovery operations, as a mobility control agent for instance, more frequently than xanthan bio polymer. The main solution property of polymer which is important in EOR process is the viscosity of the polymer.

This chapter will review the concept were used and determined in the next chapter such as the intrinsic viscosity, $[\eta]$ and effect of solvent salinity. Non-Newtonian fluid, like polymers, does not show the same viscosity at all shear rates either in capillary tubes and porous media.

In this Chapter, the rheological behavior and properties of non-Newtonian fluids in the capillary tube and porous media is discussed.

There may be significant interactions between the transported polymer molecules and the porous medium. These interactions may cause the polymer to be retained in the porous medium and will to some reduction on the rock permeability. In this chapter, mechanisms of retention such as polymer adsorption, mechanical entrapment and hydrodynamic retention will be briefly discussed.

At the end, some important aspect of behavior of polymer solutions passing through porous media will be described.

2.2 Property and bulk rheology of synthetic polymer

2.2.1 Molecular weight and intrinsic viscosity

The HPAM molecule is a flexible chain structure and it will interact strongly with ions in solution. The average weight of HPAM is typically in the range 2-10 $\times 10^6$.

The viscosity of polymer solution is related to the size of the molecule in solution. The larger the molecular, the higher the viscosity of polymer in that particular solution. It is obvious that the quantity of viscosity in the solution is related to the polymer concentration in the

solution. One of the fundamental quantity which is most related to the molecular size of the polymer in solution is intrinsic viscosity, $[\eta]$. By definition the intrinsic viscosity is the limit of the reduced viscosity or inherent viscosity as the solution concentration decreases to zero (Sorbie 1991):

$$[\eta] = \lim_{c\to 0} \frac{\eta - \eta_s}{c\eta_s} = \lim_{c\to 0} \eta_R \qquad (2.1)$$

Or

$$[\eta] = \lim_{c\to 0} \frac{ln\eta_r}{c} = \lim_{c\to 0} \eta_I \qquad (2.2)$$

Where c is the polymer concentration, η_s is solvent viscosity, η_r is relative viscosity and is equal to $\eta/\ \eta_s$, η_R is reduced viscosity and η_I is inherent viscosity.

Huggins (1942) developed the relationship between the specific viscosity and concentration of polymer for low-concentration solutions:

$$\frac{\eta_{sp}}{c} = [\eta] + k'[\eta]^2 c \qquad (2.3)$$

Where *k'* is Huggins constant which for polymers in good solution has the value 0.4 ± 0.1 (Rodriguez, 1983). Kraemer (1938) introduced another definition for intrinsic viscosity:

$$\frac{\eta_r}{c} = [\eta] + k"[\eta]^2 c \qquad (2.4)$$

Where *k"* is a constant. For good solutions the value of k" is 0.05 ± 0.05.

The rheological properties of polymer solutions, especially HPAM, may be affected by salinity and divalent-ion content. When the salt is added to polymer solution, the extension of the polymer decreases and solution viscosity declines.

2.2.2 Bulk rheology

Polymer solutions using in EOR are normally shear thinning. These solutions show Newtonian behavior at low shear rate, correspond to low flow rate, followed by region of shear thinning where the viscosity of fluid reduces, **Figure 2.1**. At very high shear rates, correspond to high flow rate, polymer viscosity tends to show second Newtonian behavior just above the solvent viscosity.

The most common relationship between shear rate and viscosity of non-Newtonian fluid is described by power law model (Bird et al., 1960):

$$\eta(\dot{\gamma}) = K\dot{\gamma}^{n-1} \qquad (2.5)$$

Where K and n are constant. For shear thinning material n is less than 1 while n is equal to 1 for Newtonian fluid.

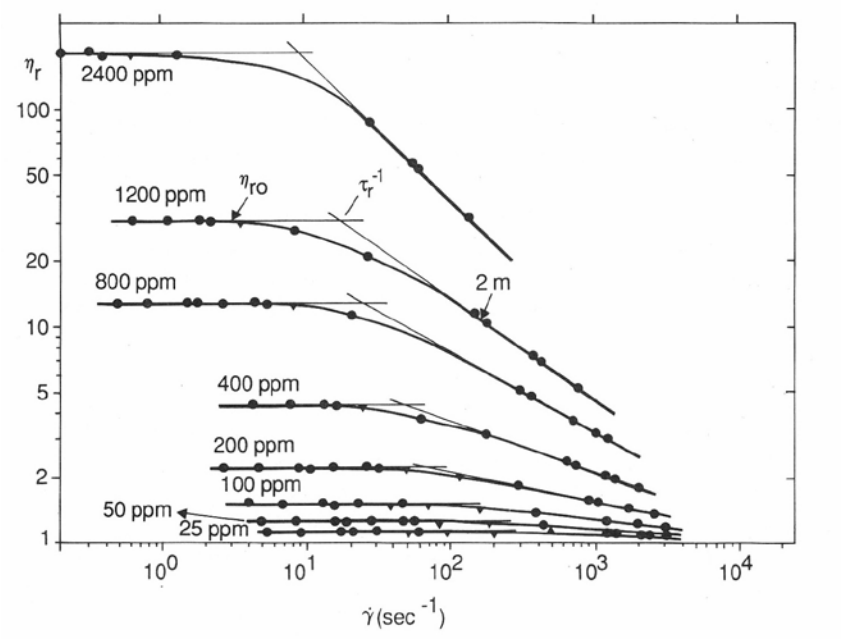

Figure 2.1 Viscosity versus shear rate of xanthan solution at a range of polymer concentration (after Chauveteau, 1982)

Where *K* and *n* are constant. For shear thinning material *n* is less than 1 while *n* is equal to 1 for Newtonian fluid.

Carreau (1972) developed the new model which the shear regimes much better:

$$\eta(\dot{\gamma}) = \eta_\infty + (\eta_0 - \eta_\infty)[1 + (\lambda\dot{\gamma})^2]^{(n-1)/2} \qquad (2.6)$$

Where η_∞ and η_0 are high shear rate Newtonian value and low shear rate Newtonian value and λ is a time constant.

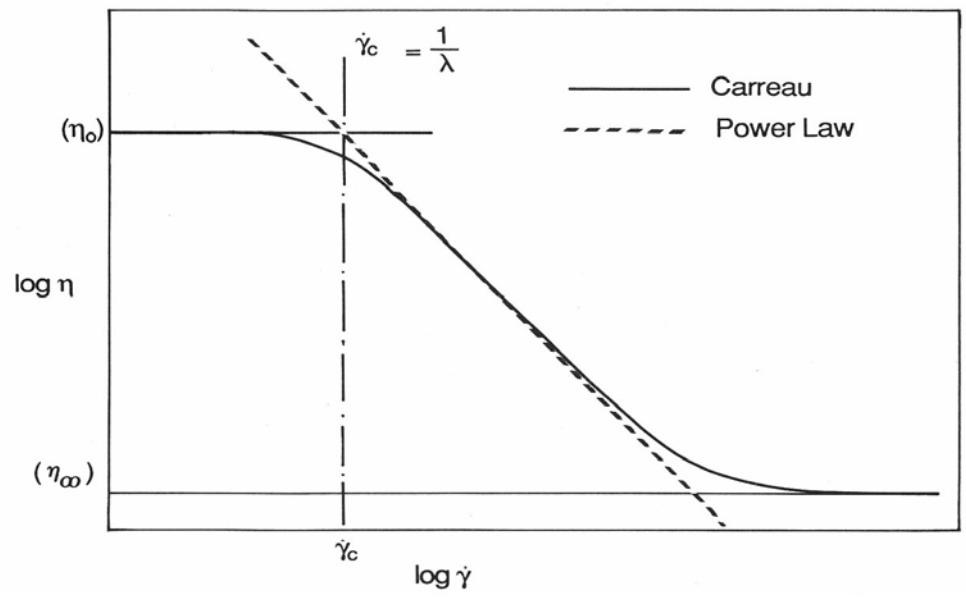

Figure 2.2 Comparision of power law model and Careau model, (after Sobbie, 1991)

Figure 2.2 compares the Careau model with power law model. It seems that Carreau model gives a much better fit to viscosity versus shear rate data.

2.3 Newtonian and non-Newtonian fluid flow through capillary tube

2.3.1 Newtonian fluid

Hagen-Poiseuille law (Bird et al., 1960) describes the flow on Newtonian fluid in tube:

$$q = \pi \frac{P_0 - P_L}{8L\mu} R^4 \tag{2.7}$$

Where *L* and *R* are the length and radius of the capillary tube and (P_0-P_L) is the pressure drop across the tube. Equation 2.7 is valid laminar flow where the Reynolds numbers is less than 2100. The volume flow rate through the capillary, *q*, can be determined from equation 2.7:

$$q = \pi R^2 u \tag{2.8}$$

Where *u* is the average velocity.

Using shear stress definition, wall shear rate for Newtonian fluid expresses with:

$$\dot{\gamma} = \frac{4u}{R} \tag{2.9}$$

2.3.2 Non-Newtonian fluid

Shear stress depends on shear rate for non-Newtonian fluid. Using the power law, The equivalent of the Hagen-Poiseuille law given earlier in equation 2.7, for non-Newtonian fluid becomes:

$$q = \frac{\pi n R^{(3n+1)/n}}{3n+1} \left(\frac{P_0 - P_L}{2KL} \right)^{1/n} \tag{2.10}$$

Where *K* and *n* are the power law constants. Typical number for *n* is between 0.4 to 0.7.

Using the same approach for Newtonian fluid, the wall shear rate for non-Newtonian fluid is (Christopher, 1965):

$$\dot{\gamma} = \left(\frac{1+3n}{4n} \right) \frac{4u}{R} \tag{2.11}$$

As $n \rightarrow 1$ the term in parenthesis go to one as well, and equation 2.11 reduces to the equation 2.9 which is for Newtonian fluid.

2.4 Polymer flow through porous media

2.4.1 Polymer retention in porous media

As mentioned in the introduction to this chapter, polymer adsorption, mechanical entrapment and Hydrodynamic retention are three main retention mechanisms of polymer retention through porous media.

Polymer adsorption

The interaction between the polymer molecules and solid surface causes polymer molecules to be bounded to the surface of the solid mainly by physical adsorption.

Basically the polymer sits on the surface of the rock, and the larger the surface area available the higher the levels of adsorption. Rocks with lower permeability have higher surface available in the porous media. Therefore the adsorption may be more in the rock with low permeability. In the rock with very low permeability, polymer may not be able to inter and adsorption will reduce. Adsorption cannot be avoided since it is between polymer rock surface and solvent. Therefore main work has been done on adsorption by many workers.

Mechanical entrapment

Retention by mechanical entrapment is occurs when larger polymer molecules trap in narrow flow channels (Willhite, 1977). Assuming porous media as a complex pore structure with large interconnected networks giving lots of possible routes which connects inlet and outlet of the core. As polymer solution passes through this complex connected network, molecules may go through any available routes and if the rout be narrow enough, polymer molecule will trap and block the rout. And probably cause more trapping at the upstream of blockage. As a consequence of this process, concentration of effluent will reach to input concentration after many pore volume of injection. And if the number of entrapment locations exceeds the critical number the core would block eventually.

Mechanical entrapment is a more likely mechanism for polymer retention for lower permeability cores where the pore sizes are small and chance of polymer molecules to be trapped is very high.

This has been studied by several workers. There are a very few workers studied retention in present of residual oil phase and most of the works has been done on water-wet cores.

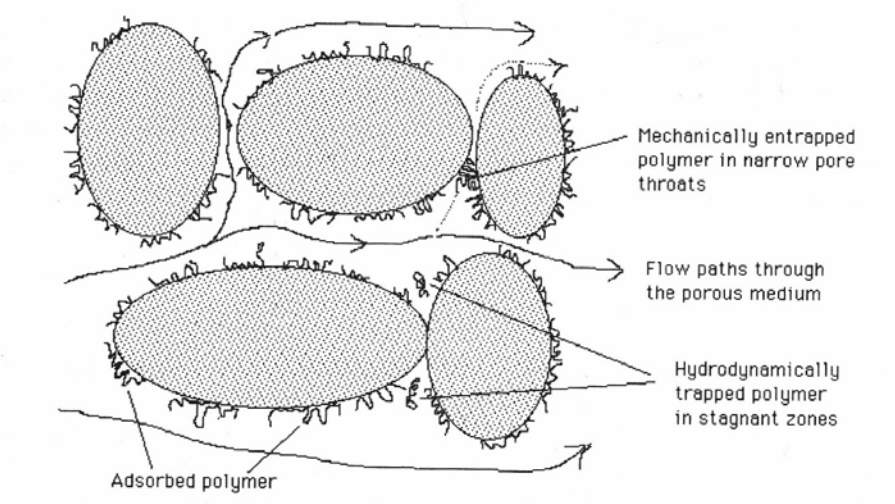

Figure 2.3 Schematic diagram of polymer retention mechanisms in porous media (after Sorbie, 1991)

Hydrodynamic retention

It has been observed that after reaching full concentration of input in effluent at constant rate, the total level of retention changed when fluid flow was adjusted to new value (Chauveteau, 1974). Although the mechanism of hydrodynamic retention is not firmly established, there is a good explanation for that. As illustrated in **Figure 2.3**, hydrodynamic drag force traps some of the polymer molecules temporarily in stagnant flow regions. In such region it may be possible to exceed the polymer stream concentration. When flow rate stops, these molecules may introduce into main stream channels and increase the concentration. When the flow starts again the effluent concentration shows a peak.

2.4.2 Polymer rheology in porous media

Polymer apparent viscosity model

Darcy law gives (Dake, 1978)a linear relationship between flow rate, q, and Pressure drop, ΔP, defining permeability as a measured parameter for conductivity of porous media as:

$$k = \frac{\mu q L}{A \Delta P} \tag{2.12}$$

Where A and L are cross sectional area and μ is Newtonian viscosity of fluid flowing through porous media.

For non-Newtonian fluid the viscosity driving from Darcy law by rearranging equation 2.12 defined as apparent viscosity, η_{app}:

$$\eta_{app} = \frac{kA\Delta P}{qL} \tag{2.13}$$

In this case η_{app} is not constant and the relationship between ΔP and q is not linear. Rheology of polymer in porous media has been described using apparent viscosity.

Shear rate of flow in porous media

Porous media is a complex network of channels and pore sizes in microscopic scale. Therefore both molecular structure of polymer and pore structure play very important role in determining rheological behavior. The simple model to describe fluid behavior in porous media is that the porous media is like a bundle of capillary tubes (Kawakami, 1932). Several worker (Hirasaki, 1974 and Teew, 1980) used this model to calculate the shear rate applying on non-Newtonian fluid flows through porous media.

Chauveteau (1982) defined active porous medium shear rate as:

$$\dot{\gamma} = \alpha' \frac{4u}{\sqrt{8k\phi}} \qquad (2.14)$$

Where α' is a shape parameter refers to characteristic of porous media u is a interstitial velocity (u = q/A) and ϕ is a porosity of porous media.

In situ rheology of polymer in porous media

There are two observations for polymer behavior in porous media. Some workers (Chauveteau and Zaitan, 1981) found that polymer has lower apparent viscosity than bulk viscosity in low shear rate. The polymer concentrations were used by these workers was less than unity (Sorbie, 1991). Other workers (Cannella et al, 1988) which used polymer concentration more than one, have shown apparent viscosity more than bulk viscosity in low shear rate.

Since HPAM has flexible coil structure shows elastic behavior. Chauveteau described the flow of HPAM in geometries varying from the very simple pure shear, through to complex mixed flow in porous media. In pure shear flows, HPAM behavior is just a shear thinning. In porous media, high flow rate applies high shear force on polymer molecule and causes the shape of polymer molecule to deform. The molecule tends to elongate passing through pore throats and channels which increases molecular size and consequently apparent viscosity increases. When the polymer molecule has been fully stretched, the force maybe large enough to break the molecule chain causing mechanical degradation. The depredated polymer has lower viscosity due to smaller size comparing with original molecule and apparent viscosity decrease.

3 Experiments

The experimental part of this work was divided into two parts. In the first part bulk rheology properties of synthetic polymers were investigated briefly. In second part, one of the diluted polymer solutions was selected to be use as the injecting fluid for conducting polymer core flood experiments.

Two types of synthetic polymers, 3630 and 3230, were selected. Four polymer solutions were made by dissolving them into two different brines namely, Synthetic Sea Water (SSW) and Nano-Filtrated Sea Water (NF-SW). Each solution was diluted into various polymer concentrations and the bulk viscosities of these diluted solutions were measured as a function of the applied shear rate.

Core flooding experiments were performed with a new set of laboratory equipments. In order to measure the effluent viscosity, a capillary tube was used immediately after the core holder and the pressure drop across the capillary tube was logged as a function of time.

Four core samples were used; two of them were Bentheim and the other two Berea sandstone core samples. The wettability of the two core samples, one of each type, was altered with Quilon to intermediate and oil wet, respectively.

3.1 Chemicals

In this assignment synthetic polymers from SNF were used. The polymers are shown in **Table 3.1**.

Table 3.1 Polymer properties.

Polymer name	Molecular weight, M_w Dalton	% hydrolysis
3630	20	30
3230	5	30

The first digit in the name of polymers refers to hydrolysis For instance, in the 3630 polymer, the firs digit, 3, refers to 30 percent hydrolysis

The polymers were dissolved in two types of brines with different salinity which the components are listed in **Table 3.2**. Synthetic sea water (SSW) was used in both bulk viscosity measurements and core flooding while nano-filtered sea water (NF-SW) was only used in viscosity measurements.

In all experiments, isopar-H, with a viscosity of 1.3 mPa.s, was used in all core samples as the oleic phase.

Table 3.2 Brine compositions and salinities.

Salt	Synthetic sea water(SSW), g/l	Nano-filtered sea water(NF-SW)
NaCl	23.495	9.686
KCl	0.746	0.000
$MgCl_2$-$6H_2O$	9.149	0.272
$CaCl_2$-$2H_2O$	1.911	0.064
Na_2SO_4	3.408	0.000
$NaHCO_3$	0.168	0.138
TDS	33.544	10.000

3.2 Bulk viscosity measurements

Different types of viscometer are currently being used to determine rheological properties of polymers. In this work, all bulk viscosities were measured using an Anton Paar MCR 301 rheometer, **Figure 3.1**. Measurements were conducted at 20^{o}C and variable shear rates ranging from 0.1 s^{-1} up to 500 s^{-1} using a cone measuring head.

Polymer viscosities were measured both at increasing and decreasing shear rate. It was found that measured viscosities were of a higher accuracy while the shear rate decreases rather than increases.

Figure 3.1 Anton Paar MCR 301 rheometer (from *www*.anton-paar.com)

3.3 Core flooding Experiments

Two Bentheim and two Berea sandstone core samples were used for core flooding experiments. Normally, both Bentheim and Berea formations are strongly water-wet. In

order to compare the polymer behavior in both oil-wet and water-wet porous media, one of each type of core samples was treated with Quilon to alter the core wettability to oil-wet (see appendix A). The relevant core properties of the various samples used in the four core flooding experiments are listed in **Table 3.3**.

Table 3.3 Core samples properties.

Core Properties	Bentheim water-wet	Bentheim oil-wet	Berea water-wet	Berea oil-wet
Diameter, cm	3.79	3.79	3.76	3.77
Length, cm	24.3	18.6	24.95	24.96
Pore volume, cm^3	58.62	38.51	63.51	60.61
Porosity, %	21.34	18.33	22.83	21.27
Permeability, md	2314	1007	842	758
S_{wi}, %	22.82	27.95	35.06	27.17
S_{or}, %	39.92	32.20	36.37	22.27

Two different pumps were used for the core flooding experiments. The first one had a maximum injection rate capacity of 20 ml/min and was used for the flooding of the Bentheim cores. Due to malfunction of this pump at the beginning of the Berea core flooding experiments, the pump was replaced with another one which had a maximum injection rate of 10 ml/min.

The capillary tube was of 1 meter length and 0.635 mm (0.025 inches) inner diameter, and as was stated above, it was added immediately after core holder with its differential pressure recorded as a function of time.

Two types of Honeywell Smart transmitters were used to measure differential pressures. The first one, with a measuring interval from 0 to 7 bar, was used to measure the pressure drop across the core holder, and the second one, with measuring interval from 0 to 1 bar, was used to measure the pressure difference across the capillary tube.

3.4 Core flooding Procedure

All experiments were conducted at ambient temperature (~20^{o}C) and a backpressure of 10 bar was applied during the flooding process.

In order to detect changes in the effluent viscosity, a capillary tube was connected to the core holder and the polymer effluent introduced to the capillary tube immediately after coming out of the core holder; the pressure drop over capillary tube was also recorded during all the experiments.

The typical core flooding procedure followed can be described as follows:

1. Mount the core in core holder and apply an overburden pressure of about 40 bar. (Pressure adjustments may be needed between floods.).

2. Vacuum the core holder, saturate the core sample with SSW and calculate its porosity. (Note: measure the weight of the core holder containing the core before and after water saturation for contingency).
3. Fill piston-cell reservoir with SSW and perform a multi-rate SSW flooding test to calculate the core sample permeability.
4. Inject isopar-H at rate of 2 ml/min and measure the water production until the pressure drop across the core remains stable (measurement of S_{wi}).
5. Inject SSW at rate of 0.9 ml/min and measure the oil production until the pressure drop across the core remains stable (measurement of S_{or}).
6. Start the polymer flooding at an initial rate of 0.2 ml/min.
7. Inject SSW at a rate of 0.2 ml/min.
8. Perform second polymer flooding starting with an injection rate of 0.2 ml/min. Inject polymer until polymer breakthrough happens and pressure drop across the core stabilizes. Having injected several pore volumes, step up the injection rate and measure any possible oil production.

In some of the core flood experiments more than two polymer flood were performed.

4 Polymer Rheology

4.1 Introduction

The viscosity behavior of synthetic polymers versus shear rate is normally described by either the power-law model or the Carreau one (Carreau, 1972). The latter is a more satisfactory model for the polymer rheological behavior.

The viscosity of a polymer solution depends on the size and the structure of the molecules in the solution. The size of the polymer molecule is inversely proportional to the salinity of solution. Intrinsic viscosity, [η], is most related factor to molecular size in solution.

Polymer 3630 has higher molecular weight than polymer 3230, (see **Table 3.1**), and as a result has more viscosity than the other one in the same solution. Salinity has the largest effect on synthetic polymers and reduces the viscosity of polymer significantly. SSW has much higher salinity than NF-SW (see **Table 3.2**). Therefore, solution of the polymer 3630 in the NF-SW has the highest viscosity while the SSW makes the viscosity of the polymer 3230, the lowest in these four solutions.

In this chapter the shear thinning behavior of synthetic polymers was studied and the effect of solution salinity in polymer solution viscosity and intrinsic viscosity was shown. All experiment data was fitted to proper model. And at the end of the chapter polymer flow in capillary tube was examined and relationship between pressure drops across capillary tube in various polymer concentrations was expressed.

4.2 Bulk viscosity versus shear rate

Two different polymer, 3630S and 3230S, were mixed in two brines, SSW and NFSW, yielding four polymer solutions that were used to study the bulk polymer behavior as a function of the applied shear rate; the shear rates varied from 0.1 s^{-1} up to 500 s^{-1}. The polymer concentrations in the four polymer solutions ranged from 100 ppm to 2000 ppm.

The SSW and NF-SW measured viscosities were 1.097 mPa-s, and 1.04 mPa-s, respectively. These two viscosity values have been used as a solvent viscosity, η_∞, for rest of measurements. The measured viscosity results were matched with a Carreau model:

$$\frac{\eta - \eta_\infty}{\eta_o - \eta_\infty} = [1 + (\lambda\dot{\gamma})^2]^{(n-1)/2} \qquad (4.1)$$

And the unknown parameters n and λ determined. Where η is viscosity of polymer solution, η_0 is zero shear rate viscosity, η_∞ is infinite shear rate viscosity, λ is a time constant and n is dimensionless constant.

Polymer 3630S in SSW

In **Figure 4.1**, all measured and matched viscosities with Carreau Model are shown and in **Table 4.1** all parameters used to match the measured viscosity values with Carreau model are listed.

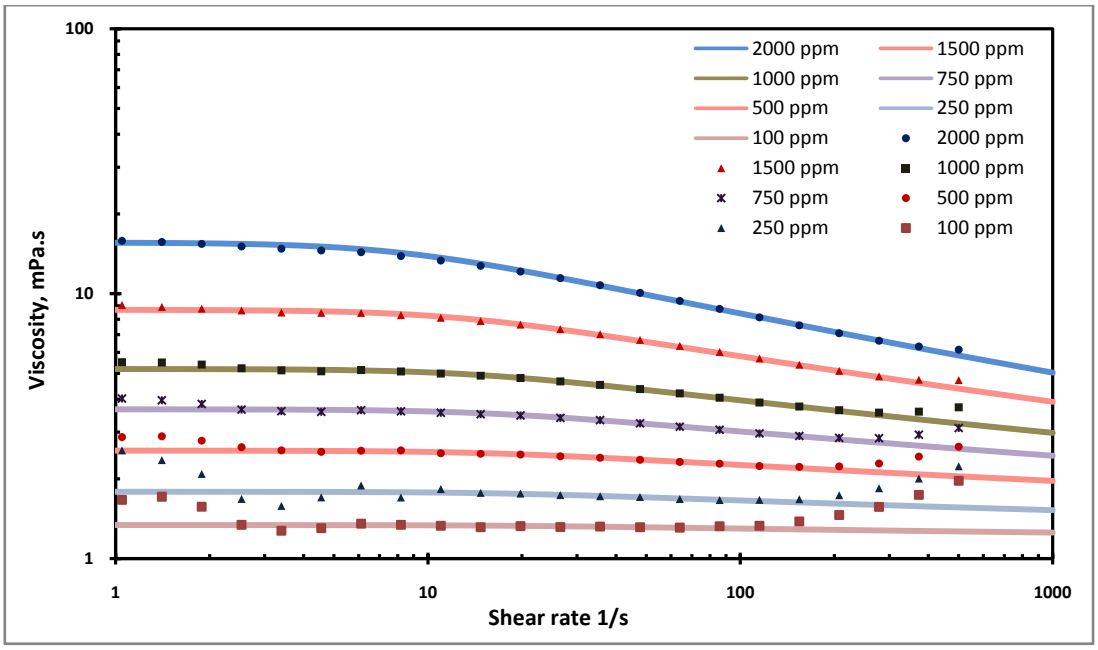

Figure 4.1 Measured and matched viscosity versus shear rate, 3630 in SSW

Table 4.1 Parameters used to match the polymer 3630 in SSW viscosity to a Carreau model

	Polymer Concentration, c (ppm)						
	100	250	500	750	1000	1500	2000
$\eta_{0,}$ mPa.s	1.339	1.787	2.556	3.66	5.2	8.7	15.6
$\eta_{\infty,}$ mPa.s	1.098	1.098	1.098	1.098	1.098	1.098	1.098
λ, s	0.053	0.056	0.061	0.063	0.071	0.083	0.125
n	0.89	0.88	0.874	0.845	0.818	0.775	0.73

Polymer 3630 in NF-SW

Comparing the polymer 3630 viscosity in the SSW and NF-SW, **Figures 4.1 and 4.2**, shows the effect of salinity on the polymer viscosity. Divalent-ion content has more effect on polymer viscosity than salinity. In addition to salinity, higher amount of divalent-ion content in SSW reduces the polymer molecule more and as a result, the viscosity of the polymer decreases enormously.

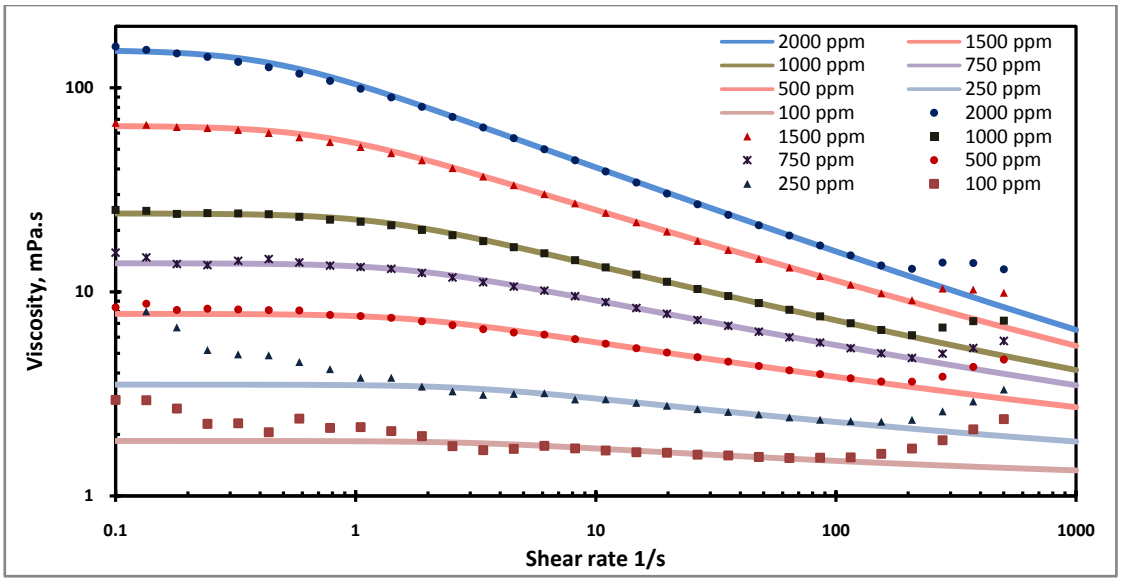

Figure 4.2 Measured and matched viscosity versus shear rate, 3630 in NF-SW

Table 4.2 shows that although the exponent constant, n, is decreasing as the polymer concentration increases, both the time constant, λ, and viscosity at zero shear rates, η_∞, increase with concentration.

Table 4.2 Parameters used to match the polymer 3630 in NF-SW viscosity with a Carreau model

	Polymer Concentration, c (ppm)						
	100	250	500	750	1000	1500	2000
η_0, mPa.s	1.86	3.51	7.8	13.8	24.2	65	153
η_∞, mPa.s	1.04	1.04	1.04	1.04	1.04	1.04	1.04
λ, s	0.294	0.313	0.556	0.588	0.781	1.389	2.273
n	0.82	0.805	0.78	0.741	0.698	0.63	0.57

Polymer 3230 in SSW

High salinity of SSW and low molecular weight of the 3230S polymer give this solution the lowest viscosities for a given polymer concentration.

The results from the viscosity measurements at low concentration and at very low shear rates should be read with care. The torque at low shear rate is very low and any small disturbance reduces the accuracy of the measured viscosity significantly.

Table 4.3 Parameters used to match the polymer 3230 in SSW viscosity to a Carreau model

	Polymer Concentration, c (ppm)						
	100	250	500	750	1000	1500	2000
η_0, mPa.s	1.2297	1.455	1.869	2.384	2.97	4.41	6.3
η_∞, mPa.s	1.098	1.098	1.098	1.098	1.098	1.098	1.098
λ, s	0.023	0.024	0.025	0.026	0.029	0.032	0.036
n	0.948	0.94	0.93	0.908	0.89	0.865	0.835

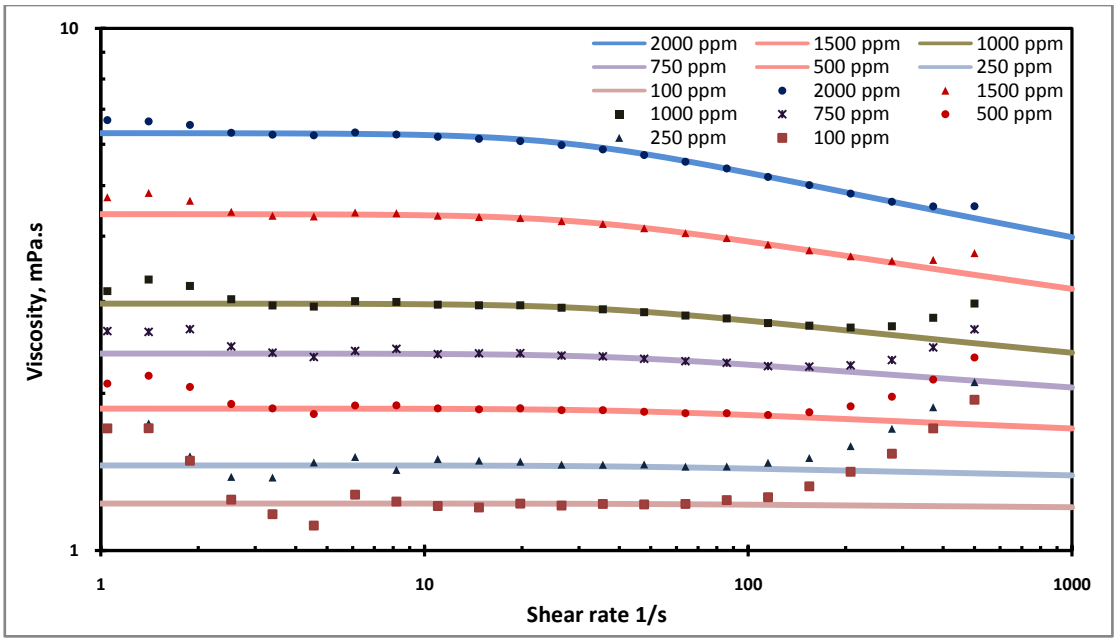

Figure 4.3 Measured and matched viscosity versus shear rate, 3230 in SSW

3230 polymer in NF-SW

There is a general trend that the bulk polymer viscosity at shear rates higher than approximately 300 s^{-1} tends to increase with increasing shear rate. This has been interpreted as experimental error due to measurement device. This error was seen in measuring SSW and NF-SW viscosities as well.

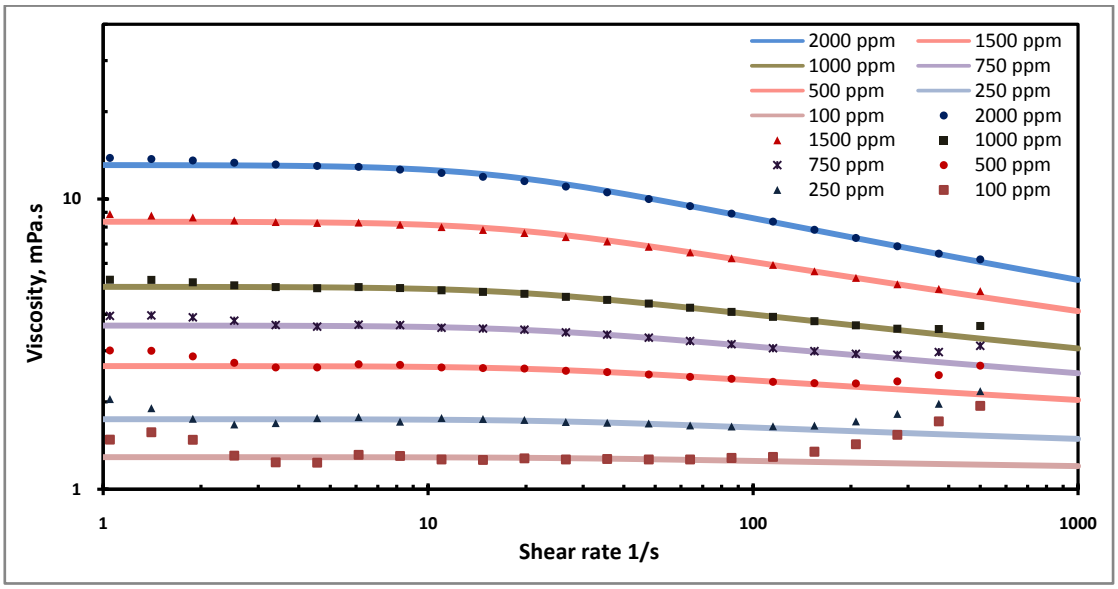

Figure 4.4 Measured and matched viscosity versus shear rate, 3230 in NF-SW

Table 4.4 Parameters used to match the polymer 3230 in NF-SW viscosity to a Carreau model

	Polymer Concentration, c (ppm)						
	100	250	500	750	1000	1500	2000
η_0, mPa.s	1.289	1.743	2.655	3.664	4.98	8.35	13.1
η_∞, mPa.s	1.04	1.04	1.04	1.04	1.04	1.04	1.04
λ, s	0.038	0.041	0.043	0.049	0.054	0.056	0.063
n	0.88	0.88	0.87	0.851	0.832	0.784	0.746

400 ppm 3630 in SSW

All polymer flooding experiments were conducted using a 400 ppm 3630 polymer concentration in a SSW solution. The Carreau model was matched on measured viscosities. In order to have better understanding of the solution flow through capillary tube, a power law model was also matched on the shear thinning part of the viscosity/shear-rate graph (see black line in **Figure 4.5**). The power law exponent has a value of n = 0.94 which is very close to 1.

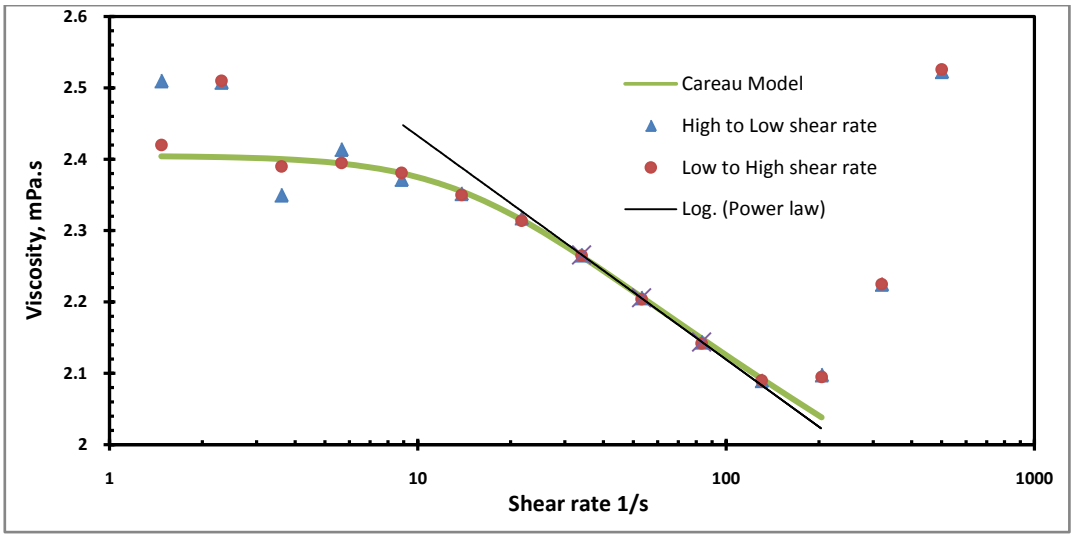

Figure 4.5 Measured and matched viscosity versus shear rate, 400 ppm 3630 in SSW

Table 4.5 Parameters used to match the 400 ppm polymer 3630 in SSW viscosity to a Carreau model

c, ppm	η_0, mPa.s	η_∞, mPa.s	λ, s	n
400	2.405	1.097	0.067	0.874

4.3 Intrinsic viscosity

In order to find the intrinsic viscosity, either the specific or inherent viscosity is plotted against polymer concentrations at low polymer concentration and is extrapolated to zero

concentration (Huggins, 1942; Kreamer, 1938). Here both methods were used and Huggins constant calculated.

The intrinsic viscosity for the polymer 3630 in SSW is calculated, as shown in **Figure 4.6**, by plotting the reduced specific viscosity against polymer concentration and extrapolating the fitted straight line to zero polymer concentration. Following this procedure, the intrinsic viscosity is calculated as $[\eta]$ = 2100 cm^3/g and the Huggins constant equal to 0.29. Extrapolation of the inherent viscosity to zero polymer concentration, in the same figure, gives $[\eta]$ = 2066 cm^3/g and Huggins constant of 0.34.

The result of second method for this particular solution has more reasonable shape and gives a better fit to calculated shear rate.

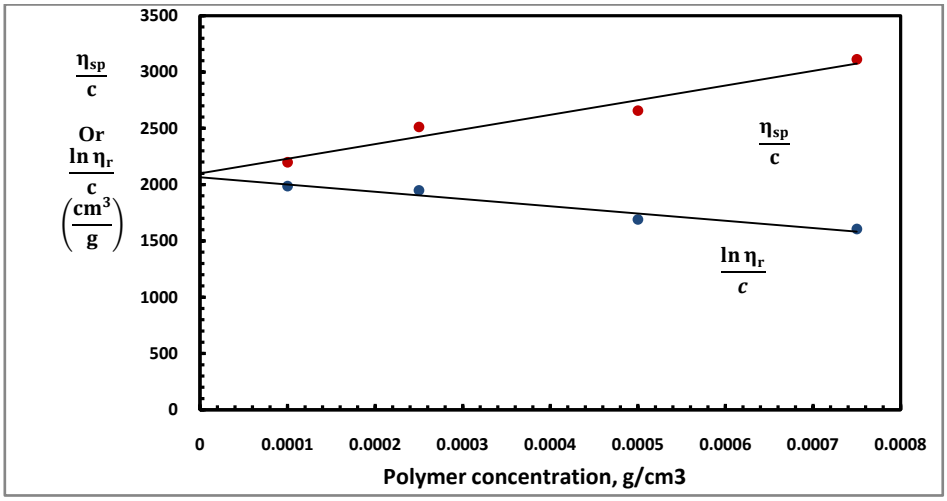

Figure 4.6 Derived Intrinsic viscosity and Huggins constant for the 3630S in SSW

Table 4.6 summarizes the calculated intrinsic viscosities and Huggins constants for all polymer solutions.

Table 4.6 Intrinsic viscosity and Huggins constant

	$[\eta]$, cm^3/g			Huggins constant		
Polymer	$\frac{\eta_{sp}}{c}$ $Vs.$ c	$\frac{\ln \eta_r}{c}$ $Vs.$ c	**Selected**	$\frac{\eta_{sp}}{c}$ $Vs.$ c	$\frac{\ln \eta_r}{c}$ $Vs.$ c	**Selected**
3630 in SSW	2100	2066	2066	0.29	0.35	0.35
3630 in NF-SW	6400	5948	6400	0.32	0.40	0.32
3230 in SSW	1154	1158	1154	0.40	0.37	0.40
3230 in NF-SW	2295	2231	2231	0.28	0.35	0.35

For many polymers in good solvents, the Haggins constant has the value 0.4 $\pm$ 0.1 (Rodriguez, 1983). In the good solvent, the polymer chains should expand and form as many contact as possible with solvent molecules (Tian Hao, 2005).

4.4 Polymer flow through capillary tube

Newtonian SSW and non-Newtonian polymer solution with 400 ppm 3630 polymer concentration were injected through a capillary tube at the various rate and ambient temperature. **Figure 4.7** shows the estimated effective viscosity versus shear rate for both fluids calculated from Hagen-Poiseuille law (Bird et al., 1960) and equation 4.3:

$$Q = \pi \frac{\Delta P}{8L\mu} R^4 \qquad (4.2)$$

L and *R* are the length and radius of capillary tube, ΔP is the pressure drop along the tube, μ is the effective viscosity and Q is injecting flow rate. The shear rate for Newtonian fluid was calculated from equation (K. S. Sorbie):

$$\dot{\gamma} = \frac{4V}{R} \qquad (4.3)$$

Where *V* is the average fluid velocity in capillary tube: $V = Q/\pi R^2$

Since the viscosity of non-Newtonian fluid changes by changing the shear rate, the fluid velocity and shear rate are not linearly dependent. Using power law expression, the shear rate for non-Newtonian fluid was become (K. S. Sorbie):

$$\dot{\gamma} = \left(\frac{1+3n}{4n}\right)\frac{4V}{R} \qquad (4.4)$$

Where *n* is power law exponent which calculated in section 4.2; n=0.938

The difference between equations 4.3 and 4.4 is the expression inside parentheses and the value of mentioned expression for 400 ppm 3630 in SSW is equal to 1.016. Using equation 4.3 to calculate non-Newtonian shear rate introduces an error of 1.63 percent that is negligible.

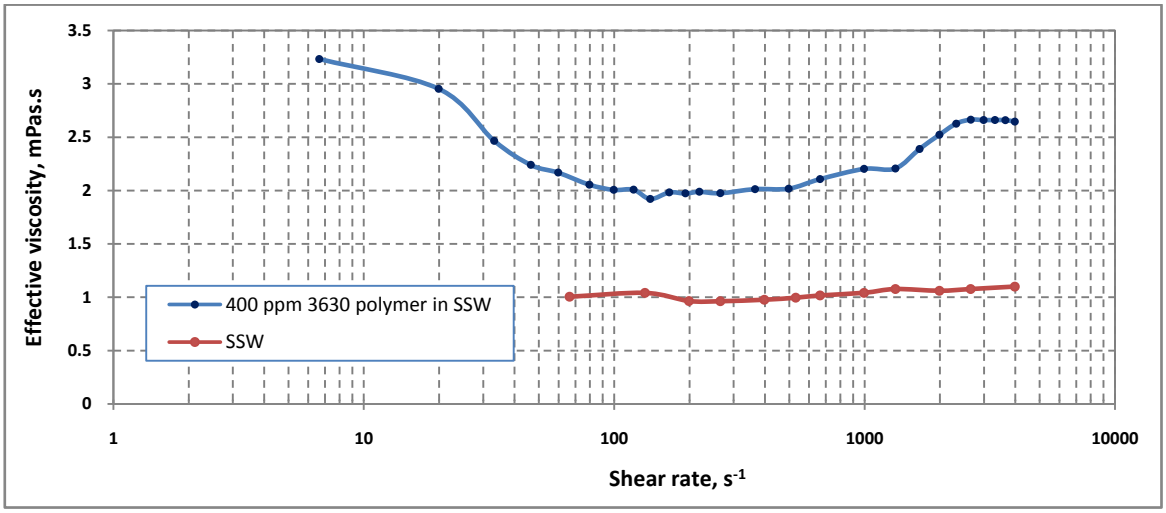

Figure 4.7 Calculated effective viscosity of SSW and 400 ppm 3630 in SSW solution in various shear rates from capillary tube flooding

According to the **Figures 4.7 and 4.8**, for shear rates less than 100 s^{-1}, (which correspond to injection rates lower than 0.15 ml/min), the polymer solution displays a shear-thinning type behavior. The same solution maintains a constant viscosity at shear rates between 100 s^{-1} and 500 s^{-1} (corresponding to injection rates of 0.15 ml/min and 0.75ml/min, respectively) and for shear rate values higher than 500 s^{-1} the calculated effective polymer viscosity increases again. For the SSW the calculated fluid viscosity appears to be constant for all injection rates, as expected. Note that most of polymer flooding experiments were performed with an injection rate of 0.2 ml/min (130 s^{-1}), which is in upper Newtonian regime and has viscosity value of η = 1.98 mPa.s, **Figure 4.8**.

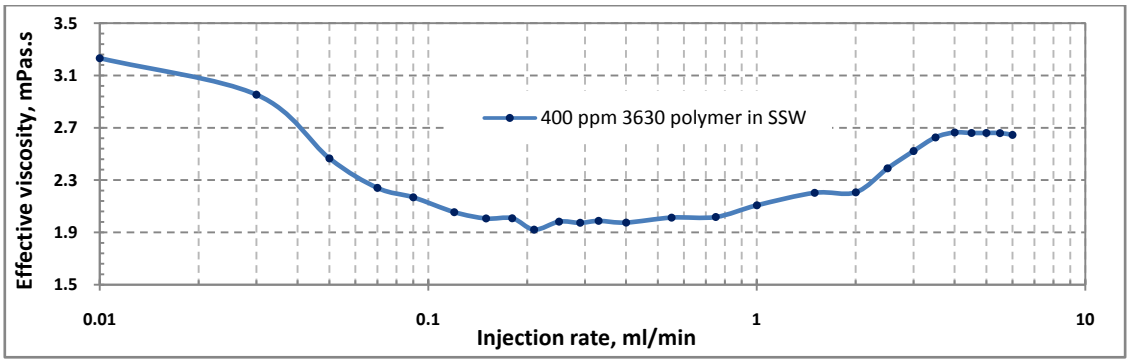

Figure 4.8 Calculated effective viscosity of SSW and 400 ppm 3630 in SSW solution in various injection rates from capillary tube flooding

The same approach which was used to calculate the intrinsic viscosity and Huggins constant for zero shear rate viscosities in section 4.3, has been used, **Figure 4.9**, to determine the viscosity of various concentrations at shear rate of 130 s^{-1} (corresponding to injection rates of 0.2 ml/min).. The value of intrinsic viscosity is constant for polymer 3630 in SSW and equal to 2066 cm^3/g, **Table 4.6**, while the new constant value, k, corresponding to shear rate of 130 s^{-1} for was determined.

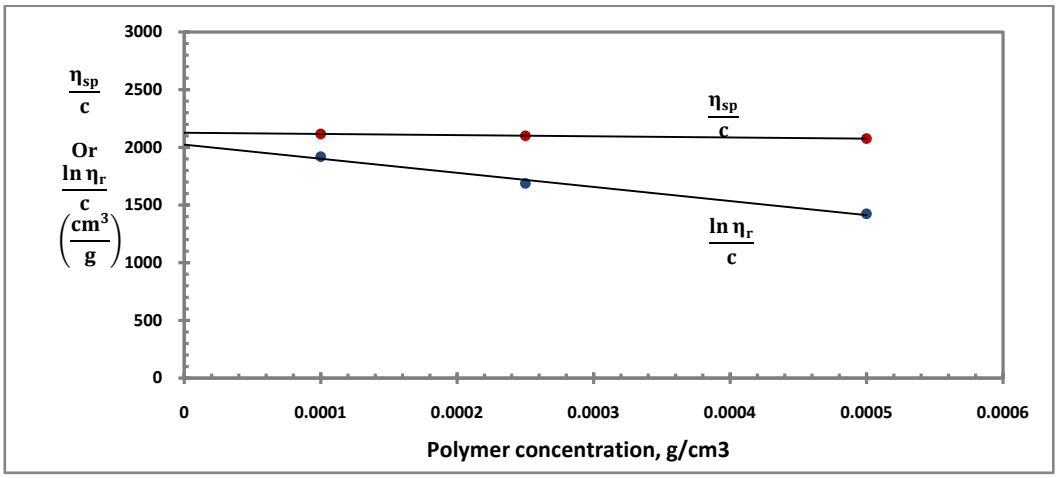

Figure 4.9 Huggins constant corresponding to shear rate of 130 s^{-1} for the 3630S in SSW

Using the Huggins (1942) formula: the relationship between the specific viscosity and concentration is as follows:

$$\frac{\eta_{sp}}{c} = [\eta] + k[\eta]^2 c \qquad (4.5)$$

Where $\eta_{sp} = \eta/\eta_s$-1 (4.6) and c is a concentration. Rearranging equation 4.5 gives the relationship between the viscosity and concentration;

$$\eta = \{[\eta]c + k[\eta]^2 c^2\}\eta_s \qquad (4.6)$$

Here k is a constant, **Figure 4.8**, with the value of k = -0.0225 and η_s is solution viscosity (SSW) with viscosity equal to 1.097 mPa.s. Inserting values of parameters, equation 4.6 became:

$$\eta = 2226.4c + 105353.7c^2 \qquad (4.7)$$

The calculated polymer solution viscosities from equation 4.7 for various 3630 polymer concentrations in SSW ranging from 400 ppm to 0 ppm, were inserted to equation 4.2 to determine pressure drop in the capillary tube for constant injection rate of 0.2 ml/min. The results are plotted against normalized concentration (c/co) in **Figure 4.10**.

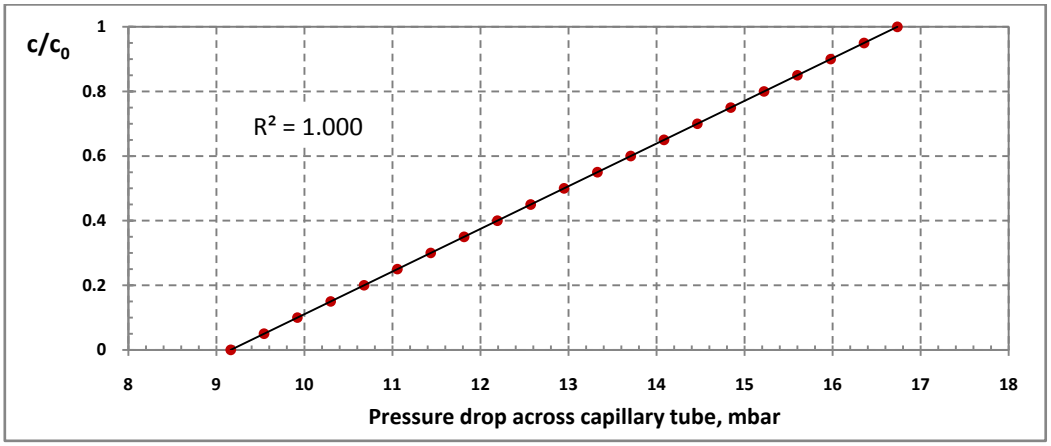

Figure 4.10 Calculated pressure drops over capillary tube versus normalized concentration of polymer solution

A linear trend line was perfectly matched on the plotted result, **Figure 4.9**. The relationship between pressure drops across capillary tube and effluent concentration is:

$$\Delta P = 7.57\, {}^{c}/_{c_0} + 9.16 \qquad (4.8)$$

Where a ΔP is in the unit of mbar. In the next chapters, change in the effluent concentration, normally at polymer breakthrough, were indicated directly from change of pressure drop across the capillary tube.

5 Polymer Flow in water wet core samples

5.1 Introduction

Berea and Bentheim water-wet cores were under investigation and the outcome is presented in this chapter. The wettability of the cores has been evaluated to compare with two other wettability-altered cores. A Series of polymer flooding have been conducted to study the polymer behavior in porous media.

5.2 Bentheim water-wet Core sample

5.2.1 Wettability

Bentheim is a highly permeable, water-wet rock (Core properties are mentioned in **Table 3.3**). Comparing wettability effect on polymer behavior in porous media, two samples of Bentheim cores were used with one of them treated with Qulian to change its wettability. In order to evaluate the effect of the Qulian treatment, wettability of cores were determined by interpretation of the oil production profile while water flooding.

SSW was used to flood the core at constant rate of 0.2 ml/min and the pressure difference across the core and amount of oil production was recorded as a function of time. Pressure was build up rapidly before SSW breakthrough due to two phase flow inside the core as shown in **Figure 5.1**.

Mobility ratio by definition (W. Green, 1998) is:

$$M = \left(\frac{k_{rw}}{\mu_w}\right)_{s_{or}} \left(\frac{\mu_o}{k_{ro}}\right)_{s_{iw}} \tag{5.1}$$

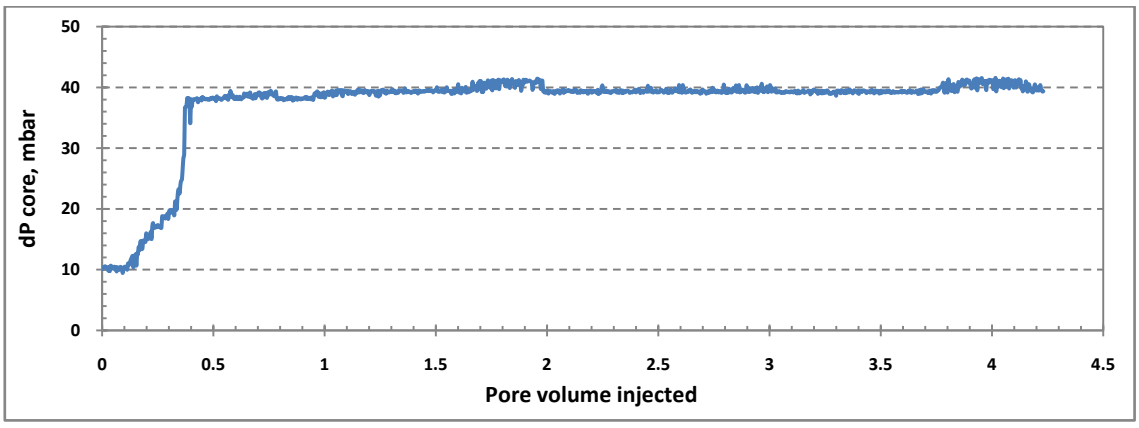

Figure 5.1 Pressure profile of SSW injection in 0.2 ml/min through Bentheim water-wet

High relative permeability of oil made the mobility ratio as small as 0.16. Breakthrough occurred after approximately 0.4 pore volume of injected SSW and after that, the pressure stabilized at approximately 40 mbar which could be interpreted as negligible change in fluids saturations in the core and thus oil production. Water effective permeability at S_{or} is equal to 219.8 md.

The oil recovery profile (see **Figure 5.2**) shows the same facts and proves the hypothesis of negligible oil production after SSW breakthrough, which is typical for water-wet cores.

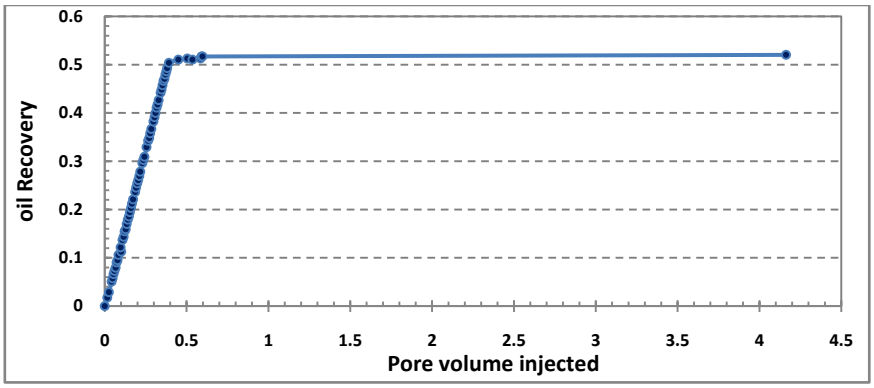

Figure 5.2 Oil recovery from SSW injection of 0.2 ml/min through Bentheim water-wet core

5.2.2 Polymer effects on porous media

Effect of polymer flooding on porous media has been investigated by a series of polymer and SSW flooding. After achieving S_{or}, the first polymer flooding at a constant rate of 0.2 ml/min was performed, followed by SSW flooding at the same rate. The second polymer flooding was started at the rate of 0.2 ml/min afterwards, flooding was continued until polymer breakthrough occurred and the difference pressure across the core and the capillary tube stabilized, then the polymer flooding was gone on in different rates. The pressure drops across the core and capillary tube were recorded in one minute per sample.

Polymer flow through a capillary tube was discussed in section 4.4; a linear relationship between pressure drop across capillary tube and polymer concentration in the solution was observed (see **Figure 4.10**). The effluent polymer concentration is linearly proportional to the differential pressure increase over capillary tube (see equation 4.8). In the other words, differential pressure profile of capillary tube has one to one correspondence to effluent polymer concentration profile. For instance, during breakthrough polymer starts to come out of the core and increases effluent viscosity, therefore pressure difference across the tube increases. Assume having homogenous dispersion of polymer in water at polymer front, breakthrough happens when 50 percent of polymer comes out of the core (W. Grean, 1998). Therefore the pressure drop across the core increase 50 percent of the time when concentration of polymer is 100 percent in effluent. The conclusion of above discussion is

that in this work, the change in the effluent concentration, normally at polymer breakthrough, were indicated directly from change of pressure drop across the capillary tube.

Polymer retention

Polymer started retaining when polymer solution entered the porous media for the first time. Therefore, polymer retention in the first polymer flooding delayed polymer breakthrough significantly. Since all retention was accrued during first polymer flooding, polymer breakthrough in the second polymer flooding happened much faster than first polymer flooding. The amount of polymer retained in porous media was calculated by comparing polymer Breakthroughs in the first and second polymer flooding.

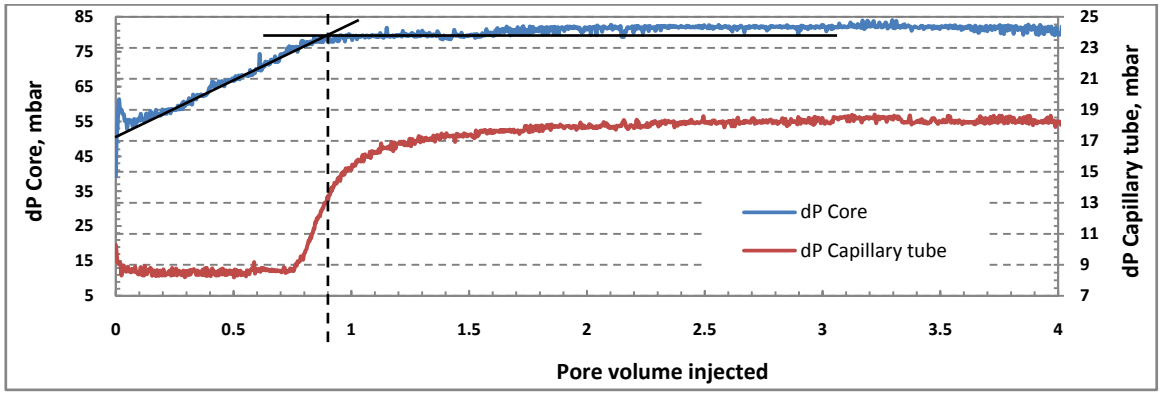

5.3 Polymer breakthrough in the first polymer flooding through Bentheim water-wet core

From the results shown in **Figure 4.9**, and above discussion, a pressure drop of 13.5 mbar corresponds to a c/c_0 value of 0.5, indicates the breakthrough of the polymer. Graphical illustrations in **Figures 5.3 and 5.4** also show that polymer breakthrough happened when the effluent polymer concentration reached to 50 percent of injection polymer concentration.

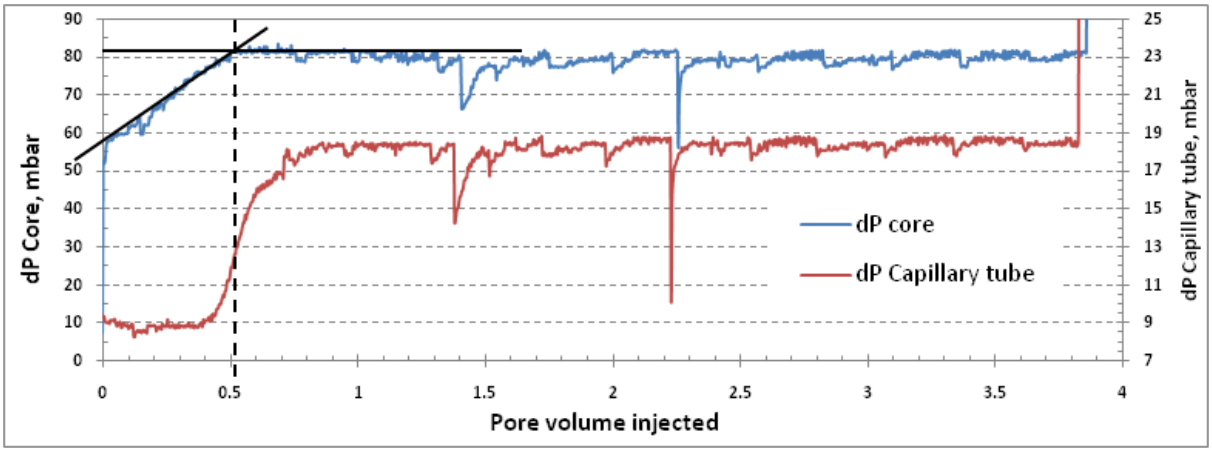

5.4 Polymer breakthrough in second polymer flooding through Bentheim water-wet core

Polymer breakthrough happened after injection of 0.905 and 0.525 pore volumes in the first and second polymer flooding, respectively (see **Figures 5.3 and 5.4**). Therefore 0.38 pore

volume of polymer was retained inside the core. Given that the actual pore volume of the core is 58.62 cm^3, and core sample weight of 567.81 g, 15.7 micrograms of polymer per gram of the core was retained.

Inaccessible pore volume, IPV

Solutions of typical water flooding polymers do not flow through the entire connected pore volume in porous media. The remainder of the pore volume is inaccessible to polymer. This inaccessible pore volume, IPV, is occupied by water that contains no polymer. This allows polymer concentration to be propagated through porous media more rapidly than water does. (Dawson, 1972)

In order to determine the IPV, SSW flood was performed after the first polymer flooding and followed by a second polymer flooding both with rate of 0.2 ml/min. SSW breakthrough occurred after 0.545 pore volume injection as shown in **Figure 5.5** and polymer breakthrough was after 0.525 pore volume of polymer injection (see **Figure 5.4**). Therefore polymer has earlier breakthrough by 0.02 pore volume, in other word, two percent of pore space is inaccessible for polymer.

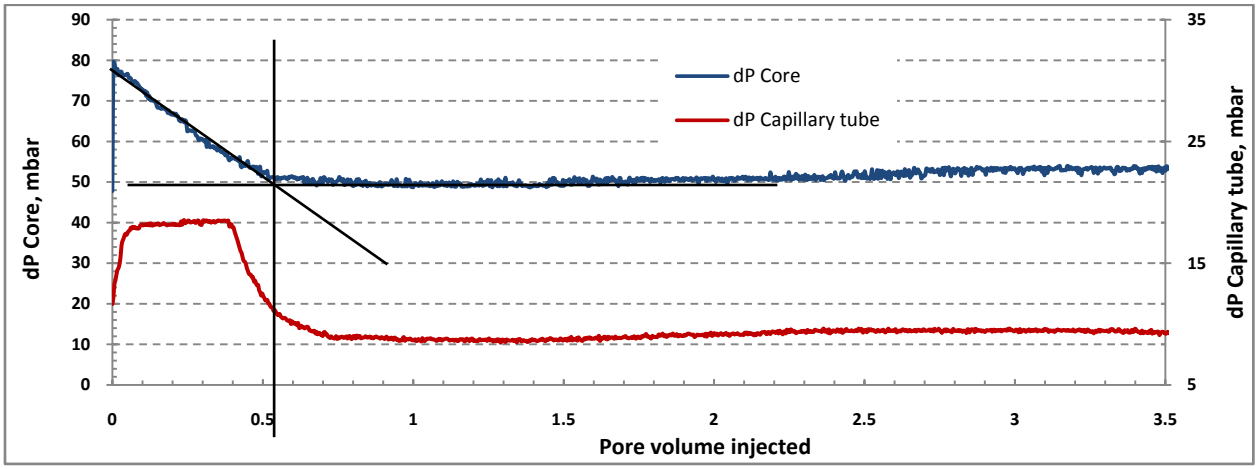

5.5 Water breakthrough in water flooding after first polymer flooding through Bentheim water-wet core

The water viscosity is lower than polymer viscosity. Therefore, during SSW flooding, water may finger into polymer solution and water breakthrough happens earlier This may introduces an error to IPV calculation and reduces the amount of calculated IPV.

A second approach to determine IPV is as follows. The amount of pore volume where water flows through is $(1-S_{or}) = 0.6$. Since, in this study all saturation values are determined using fluid injection which flows through connected porous media and assuming piston like displacement, water breakthrough is actually after 0.6 pore volume of SSW injection. As it was mentioned, the polymer breakthrough after 0.525 pore volume injection. Therefore 7.5 percent of pore volume is inaccessible for polymer to flow through.

The assumption in second approach is true in core flooding, so the second approach to calculate IPV is more accurate than first one.

Regardless of which method used for calculating IPV, the amount of IPV is low. There could be several reasons for this observation. For example, the core sample has a high permeability so the pore throat size is big which decrease mechanical entrapment inside the core. Moreover 40 percent of the core is occupied by oil that is not accessible for aqueous phase.

Permeability reduction

To determine the effect of polymer retention on permeability of core the appropriate way is to calculate the residual resistivity factor, R_{rf}, which is the ratio of the mobility of water before and after the polymer flooding (Sorbie, 1991). It can also be expressed as the ratio of the permeability of water initially and after polymer injection.

Figures 5.1 and **5.5** show water flooding stabilized pressure difference across the core, before and after polymer flooding; there is approximately 10 mbar increase in the reading pressure after polymer flooding. Having pressure difference (**Figure 5.1** and **5.5)** and core properties (**Table 3.3**) water effective permeability can be easily calculated which are 220 md and 157 md before and after polymer flooding respectively. This gives R_{rf} factor of R_{rf} = 1.39.

The low amount of R_{rf} shows that polymer retention had a small effect on water permeability. As explained above, most of the pore throats inside the core are too big to be blocked by polymer. Therefore both R_{rf} and IPV factors were small.

5.2.3 Apparent viscosity and resistance factor

Apparent Viscosity

As a part of the second polymer flooding, a multi rate flooding was performed. The capillary tube was bypassed before increasing the injection rate to 9.6 ml/min (**Figure 5.6**). The reason is because the pressure difference over the capillary tube would exceed the transmitter upper limit, if the rate increased that high. Oil was produced after the rate was increased to 3.2 ml/min. Oil production, apparent viscosity and other parameters for second polymer flooding are shown in **Table 5.1**.

For flow of polymer solution as a non-Newtonian fluid in porous media, Darcy law was used to calculate apparent viscosity, η_{app}. Where ΔP (pressure difference across core) is not a linear function of the injection rate (q).

$$\eta_{app} = \frac{kA\Delta P}{qL} \qquad 5.1$$

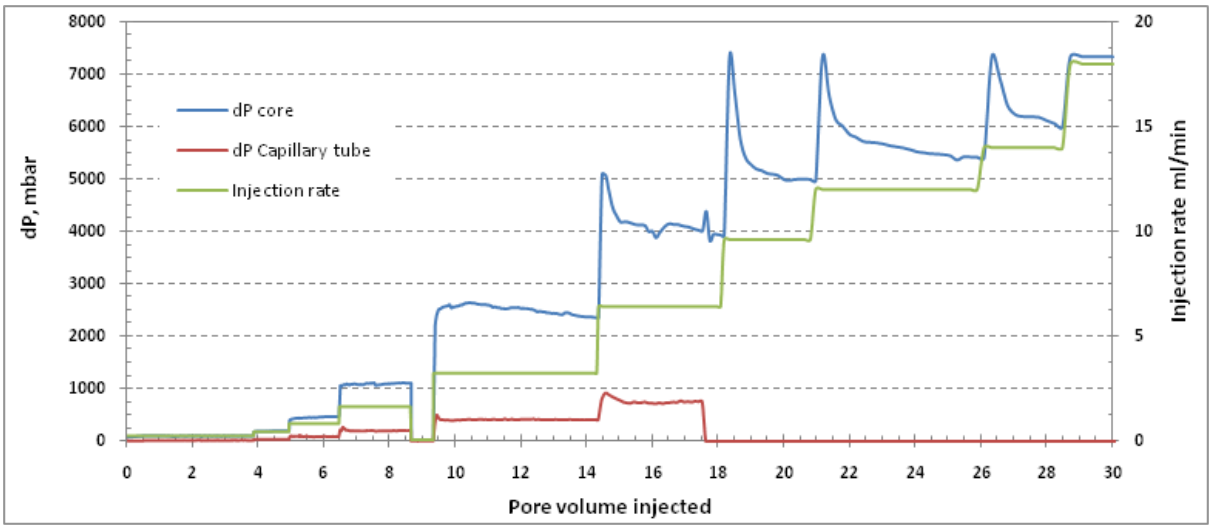

Figure 5.6 Multi rate Polymer flooding through Bentheim water-wet core

Various approaches to modeling of shear rate for non-Newtonian fluids in porous media were attempt by several workers (Zaitoun, 1981 and Christopher, 1965). Here the expression for shear rate, which has defined by Chauveteau (1981) was used.

$$\dot{\gamma}_{pm} = \alpha \frac{4u}{\sqrt{8k\phi}} \qquad 5.2$$

Where u is an interstitial velocity and α is a shape parameter characteristic of the pore structure which was determined experimentally (Stavland, 2010).

The determined value for α reported by Stavland for both the Bentheim and Berea cores is equal to 2.5.

Polymer retention and oil production could be the two important factors having an effect on effective permeability. Polymer retention may reduce effective permeability by blocking pore throats and oil production may increase effective permeability by increasing the water saturation inside the core.

The permeability, k, which is used to calculate the apparent viscosity and shear rate (using Equations 5.1 and 5.2) was the effective permeability of SSW (157 md) after polymer flooding in order to reduce the effect of polymer retention on SSW permeability. This value was kept constant in calculating apparent viscosity and shear rate for all injection rates (**Figure 5.7)**. Measured bulk viscosity and its fitted Carreau model is also depicted in **Figure 5.7.**

Table 5.1 Apparent viscosity from Darcy law in second polymer flooding

Injection rate ml/min	dP core mbar	shear rate 1/s	Apparent viscosity mPa.s	oil Production ml	Resistance factor, F_r
0.01	4.9	2.9	2.126	0	2.49
0.2	79	57.2	1.714	0	2.01
0.4	176	114.5	1.909	0	2.24
0.8	448	229.0	2.430	0	2.85
1.6	1092	457.9	2.961	0	3.47
3.2	2349	915.9	3.185	1.1	3.74
6.4	3918	1831.8	2.656	3.6	3.12
9.6	4970	2747.6	2.246	2.8	2.64
12	5400	3434.6	1.952	1.2	2.29
14	6000	4007.0	1.859	-	2.18

Figure 5.8 compares the apparent viscosity with resistance factor. Comparing apparent viscosity and Careau model in Figure 5.7 shows that the point with the lowest shear rate (calculated in rate of 0.01 ml/min) is in upper-Newtonian regime with apparent viscosity of 2.126 mPa.s. It also has lower apparent viscosity than bulk viscosity for upper–Newtonian regime. Apparently that shear thinning regime is between this point and the next apparent viscosity (calculated in rate of 0.2 ml/min). In the range of 100-1000 s^{-1} shear rate, (from the rate of 0.4 ml/min to 3.2 ml/min), apparent viscosity increases by increasing shear rate. For shear rates higher than 900 1/s (rates higher than 1.6 ml/min) oil production may increase effective permeability which should be considered. It seems that the last four points are in polymer degradation regime in which by increasing injection rate, more oil was produced and the water saturation and permeability were also increased. Therefore more error was introduced to calculation of apparent viscosity and shear rate.

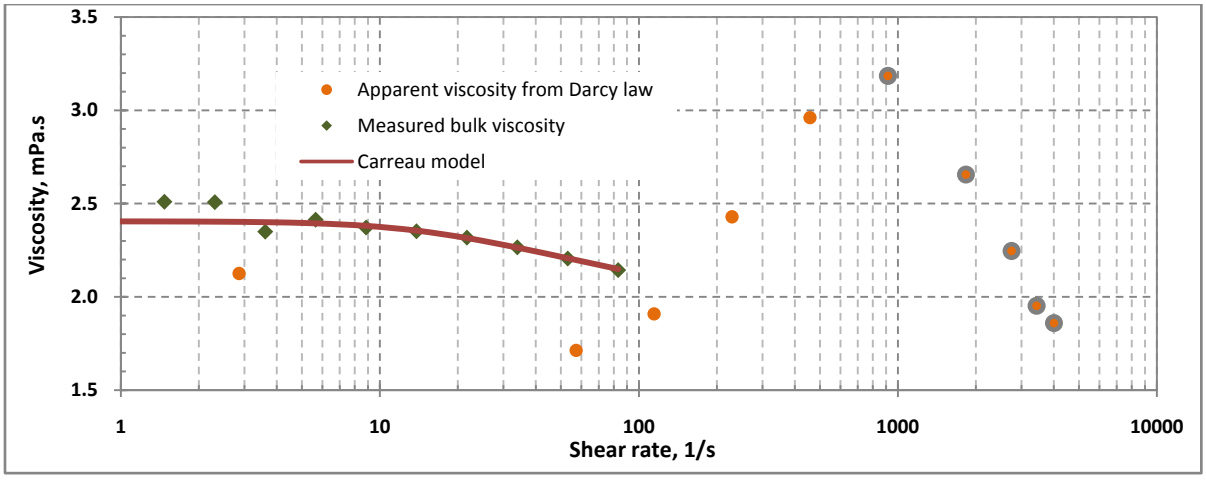

Figure 5.7 Darcy apparent viscosity and Carreau model for bulk viscosity, Bentheim water-wet core

Resistance factor Fr

Resistance factor, Fr, by definition is the ratio of the brine mobility in the porous media before polymer contact to the polymer mobility in the same porous medium (Littmann, 1988).

In **Figure 5.8**, F_r very clearly follows the same trend with the apparent viscosity as a function of injection rate. It seems that for rates less than 3.2 ml/min the only factor affecting resistance factor was water viscosity. For the rates higher than 1.6 ml/min, oil production caused an increase in the water permeability; both polymer viscosity reduction and permeability increase cause the polymer mobility and F_r to also decrease.

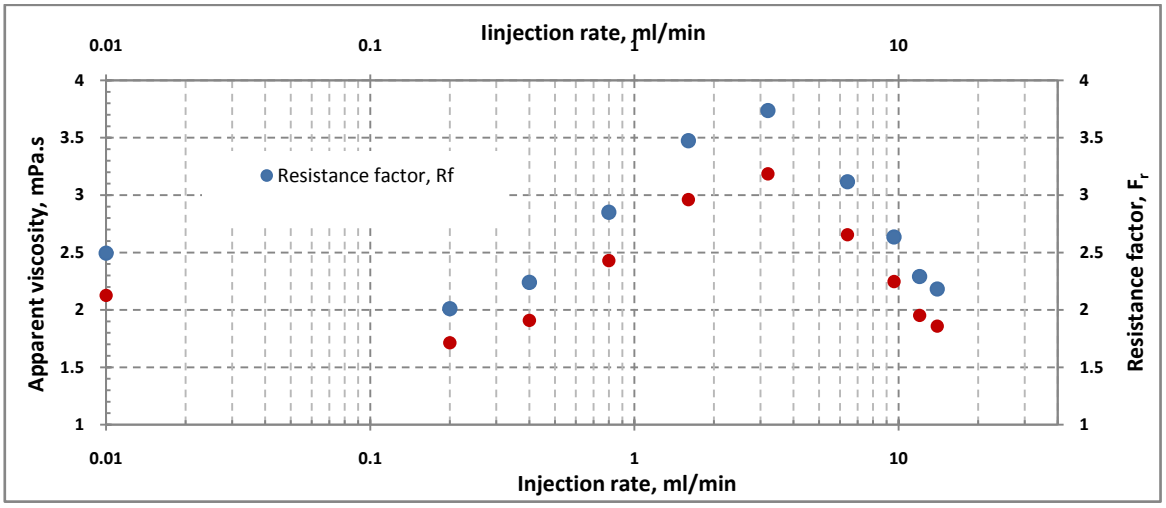

Figure 5.8 Resistance factor and apparent viscosity

5.3 Berea water-wet Core sample

5.3.1 Wettability

Berea is a water-wet sandstone rock (Core properties are mentioned in **Table 3.3**). Comparing wettability effect on polymer behavior, two samples of Berea cores were used which one of them were treated with Qulian to change the wettability of the core. In order to check the effect of the Qulian treatment, wettability of cores were checked by interpretation of the oil production profile while water flooding.

SSW was flooded with favorable mobility ratio of 0.14 and at constant rate of 0.9 ml/min and the pressure difference across the core and amount of oil production was recorded as a function of time. Pressure was build up rapidly before SSW breakthrough due to two phase flow inside the core as shown in **Figure 5.9**. Breakthrough happened after 0.46 pore volume injection of SSW. After SSW breakthrough, the pressure stabilized at 640 mbar (**Figure 5.10**) and only a very small amount of oil was produced. The oil recovery profile shows a very clear behavior of water-wet core.

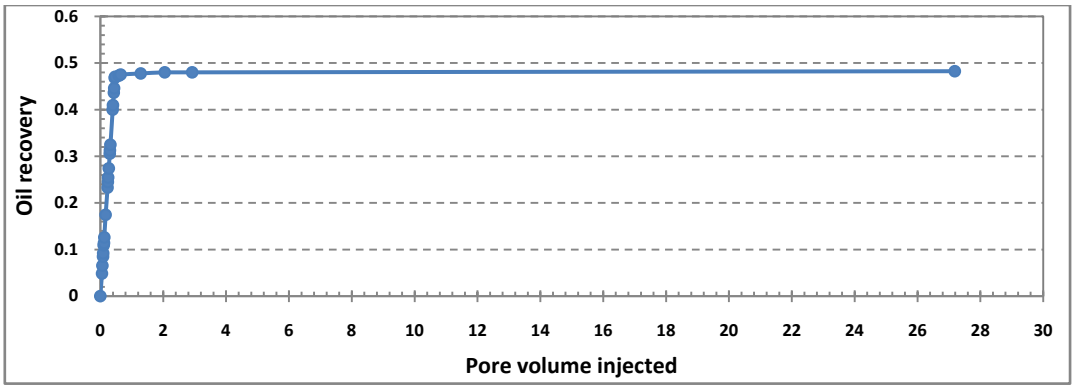

Figure 5.9 Oil recovery of SSW injection in 0.9 ml/min through Berea water-wet core

The other way to determine the wettability of a core is to plot the water production during oil flooding to achieve S_{wi} in the core. The general idea is that by injecting the wetting phase and producing the non-wetting phase, the production profile will be similar to **Figure 5.9**, which means water, i.e., the wetting phase, will breakthrough later than when the core is oil wet, and most of the oil as non-wetting phase will be produced before breakthrough. On the other hand by injecting non-wetting phase, water for oil-wet core or oil for water-wet, wetting phase will breakthrough faster and there will be a production of wetting phase after breakthrough. In this case the water-wet core was flooded by oil in order to measure S_{wi} which can be used to verify wettability of the core.

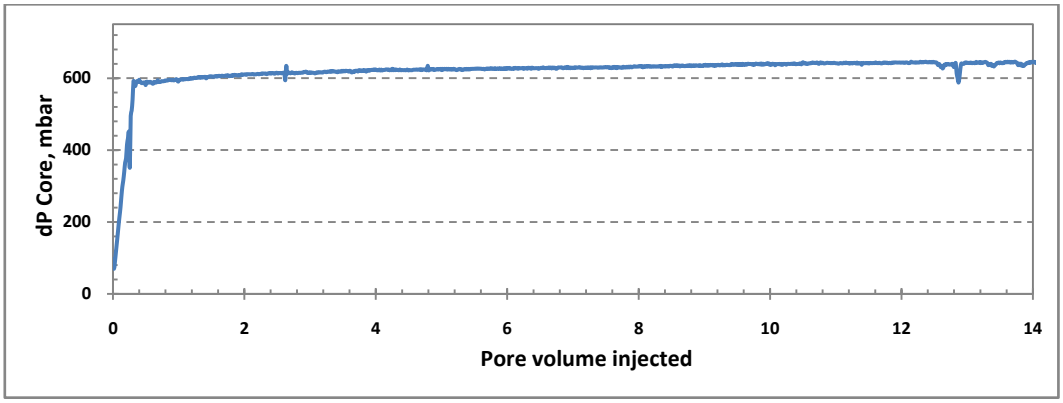

Figure 5.10 Pressure profile of SSW injection in 0.9 ml/min through Berea water-wet

Oil was flooded at the constant rate of 2 ml/min. The water production profile, **Figure 5.11**, shows that 12 ml of water were produced after oil breakthrough which occurred after injection of 0.62 pore volume of oil.

Pressure reduction after breakthrough, **Figure 5.12,** is a good indicator of an increase in the oil saturation as result of water production inside the core.

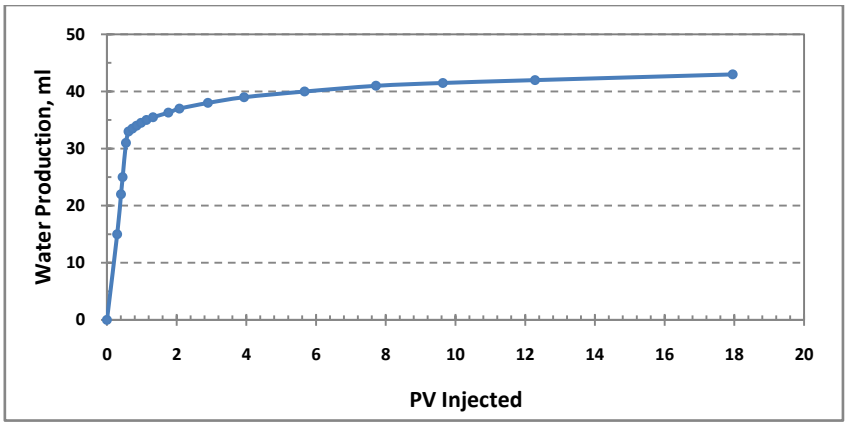

Figure 5.11 Water production, Brea water-wet

The results from both methods show that the Berea core sample is water-wet.

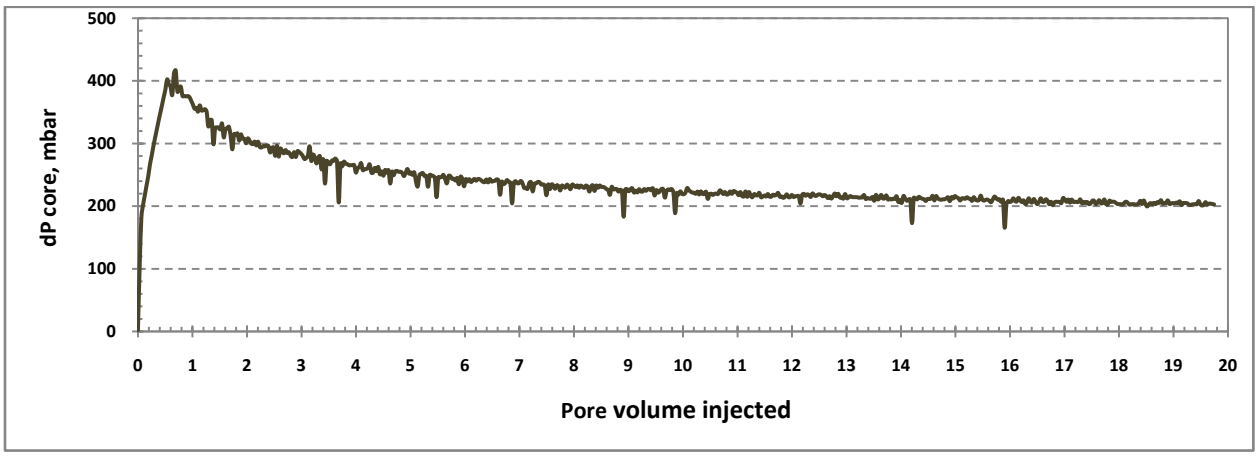

Figure 5.12 Pressure profile of oil injection in the rate of 2 ml/min through Berea water-wet

5.3.2 Polymer effects on porous media

Polymer retention

The pressure differences across both core and capillary tube in the first and the second polymer floods are plotted in **Figures 5.13** and **5.14** with injection rate of 0.2 ml/min. It seems to be very difficult to determine the polymer breakthrough from the pressure drop across the core. Therefore pressure profile of capillary tube is used to determine the breakthrough time. Breakthrough occurs when the capillary pressure is equal to the average value of pressure before and after breakthrough, 16 mbar for the first and 13.5 mbar for the second polymer flooding. The reason that these values are not equal is due to the fact that the transmitter had different calibration for each case.

Note that as stated in section 4.4, the average pressure is associated with the polymer solution with concentration of 50 percent to injecting solution concentration.

Polymer breakthrough happened after injection 1.431 and 0.487 pore volumes for the first and second polymer floods, respectively. Therefore polymer solution of 0.944 pore volume was retained inside the core. Given that the pore volume of the core is 63.51 cm^3, and core sample weight 388.97 g, 61.65 micrograms of polymer per gram of the core was retained inside the core.

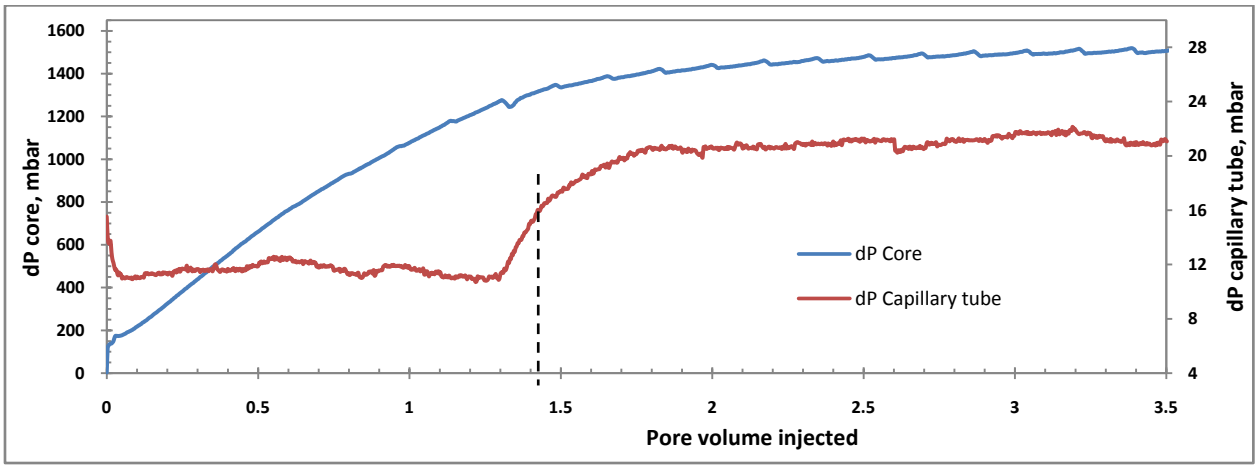

5.13 Polymer breakthrough in the first polymer flooding through Berea water-wet core

It seems that the core adsorbed a large amount of injected polymer yielding a large amount of IPV and significant reduction of the water permeability.

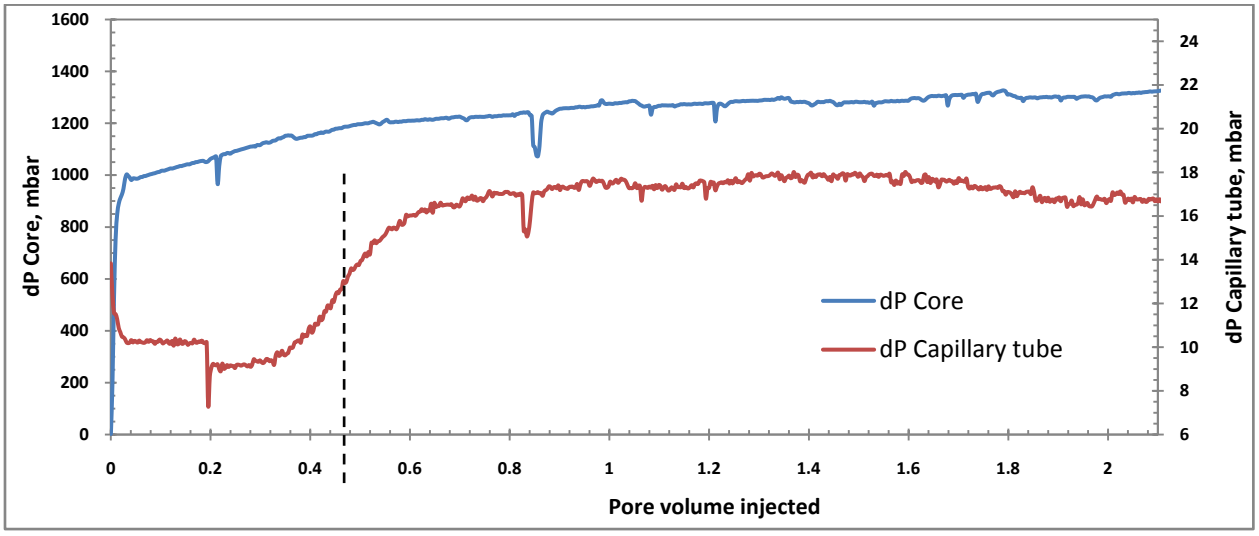

5.14 Polymer breakthrough in the second polymer flooding through Berea water-wet core

Inaccessible pore volume, IPV

The amount of pore volume available for the water to flow through is $(1-S_{or})$ = 0.636. This means that the water breakthrough occurs after 0.63 pore volumes of water injection (assuming piston-like displacement). Polymer breakthrough in the second polymer flooding

experiment happened after 0.487 pore volumes of polymer injection. Therefore the IPV value is 14.9 percent of pore volume.

Permeability reduction

The pressure difference across the core in water flooding experiments, before and after polymer flooding, changed significantly. The effective permeability was decreased from 61.7 md to 7.2 md, which gives an R_{rf} factor a value of 8.56.

While only 63 percent of pore volume was open for polymer solution to flow, a large amount of polymer retained inside the core and reduced the effective permeability significantly.

5.3.3 Apparent viscosity and resistance factor

Apparent Viscosity

After second polymer flooding, multi rate polymer flooding was performed. The injection rates and pressure drop across the core are plotted in **Figure 5.15**. Oil production, apparent viscosity and other parameters related to the second polymer flooding are shown in **Table 5.2.**

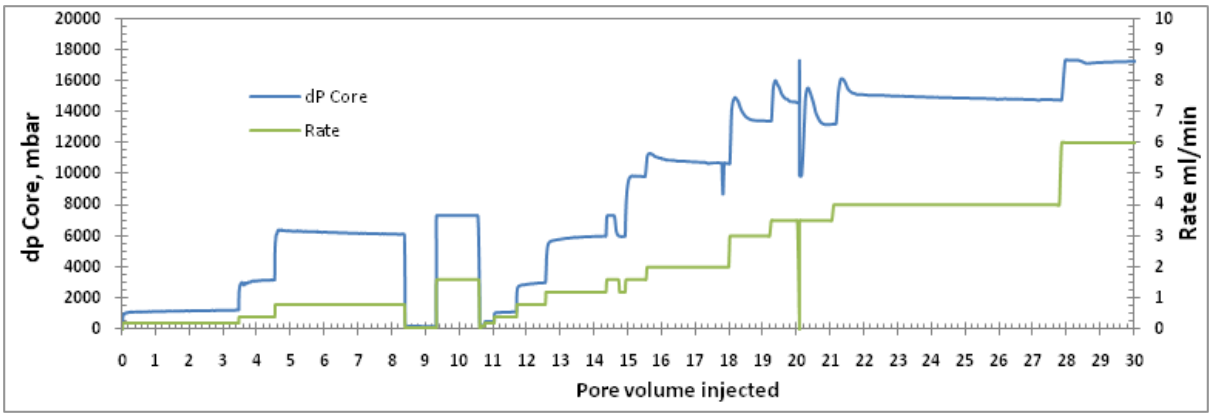

Figure 5.15 Multi rate Polymer flooding

Oil was produced after stepping up the rate to 0.8 ml/min (third injection rate). This early production of oil increased water permeability significantly. Comparing pressure difference across the core for the rate of 0.2 ml/min at the early part of the flooding, with the same rate after 11 pore volumes of polymer injection, shows drastic pressure drop which was due to oil production in the this period. All apparent viscosities were calculated based on water effective permeability from water flooding, which was performed after the first polymer flooding. Increasing the water permeability during polymer flooding due to oil production, introduced an error to apparent polymer viscosity calculation. The reason to calculate apparent viscosities was to observe the trend and study the polymer behavior inside the core.

Table 5.2 Multi rate polymer flooding parameters

Injection rate ml/min	dP core mbar	dP Capillary tube mbar	Apparent viscosity mPa.s	oil Production ml	Resistance factor, F_r
0.2	1502	22.4	1.432	0	11.00
0.4	3190	51	1.521	0	11.68
0.8	6145	74.2	1.465	0.7	11.25
0.05	195	4.9	0.744	1.3	5.71
1.6	7348	135	0.876	0	6.73
0.05	195	5	0.744	0	-
0.1	264	9.1	0.503	0	3.87
0.2	507	17	0.483	0	3.71
0.4	1125	34	0.536	0	4.12
0.8	3021	73	0.720	0	5.53
1.2	6012	132	0.955	0	7.34
1.6	9855	157	1.175	0.3	9.02
2	10700	187	1.020	1.3	7.84
3	13440	264	0.854	0.3	6.56
3.5	14671	309	0.799	0.6	6.14
4	14797	351	0.706	1.6	5.42
6	17255	537	0.548	0.8	4.21

Calculated apparent viscosity as a function of polymer injection rate was shown in **Figure 5.16.** It seems that the values of the apparent viscosities were much lower than the bulk viscosities. The error is high but the trend may give a good clue to figure out the behavior of polymer. Apparent viscosity shows the shear thickening up to the maximum value which is associated with the rate of 1.6 ml/min. It seems that polymer started to degrade afterwards

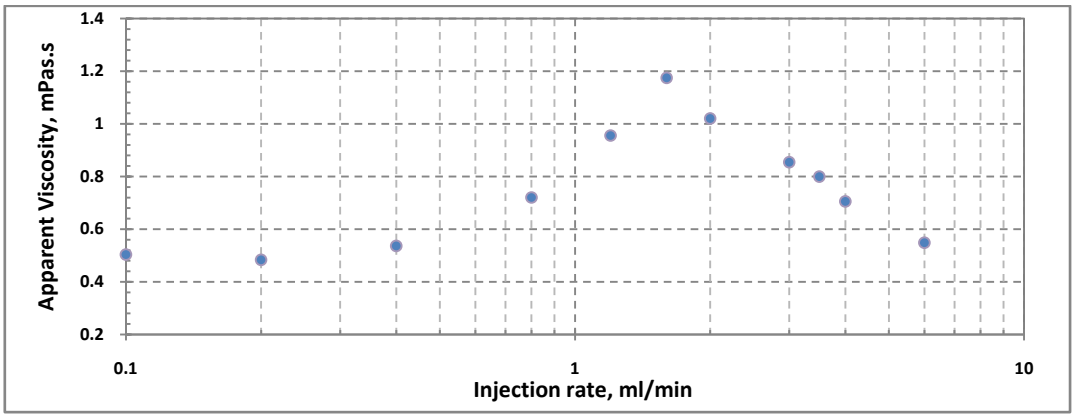

Figure 5.16 Calculated apparent viscosity in the core versus polymer injection rate

Polymer degradation decreases the polymer viscosity which could be investigated by checking the pressure drop across the capillary tube. Effective viscosities of injection polymer solution and effluent fluid in the capillary tube are plotted in **Figure 5.16**. It appears that polymer effective viscosities did not follow the injection polymer solutions' apparent viscosity after the injection rate of 1.6 ml/min. This fact is in good agreement with the statement above.

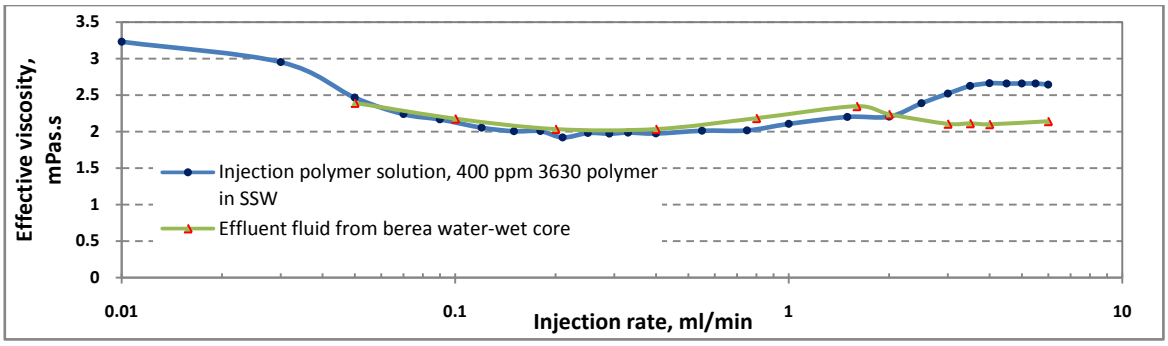

Figure 5.16 Effective viscosities of injection polymer solution and effluent fluid in Capillary tube, Berea water-wet core

Resistance factor Fr

Both resistance factor and apparent viscosity were plotted on **Figure 5.17** against polymer injection rate. The brine mobility before polymer flooding was constant. Therefore the only factor affecting F_r was polymer mobility. Although the value of the calculated apparent viscosity was based on constant permeability, it seems good agreement between apparent viscosity and resistance factor.

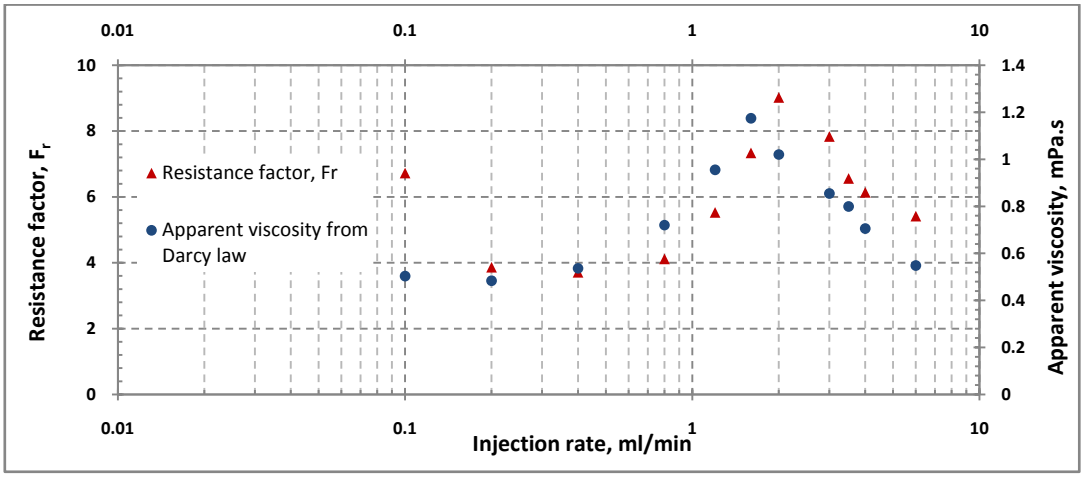

Figure 5.17 Resistance factor and apparent viscosity, Berea water-wet core

According to resistance factor in **Figure 5.17**, flooding with rate of 2 ml/min gives the lowest mobility to the polymer solution. Comparing both in rates of 0.1 ml/min and 0.2 ml/min shows that the lower mobility of polymer in the rate of 0.1 ml/min was mostly because of water permeability increase during oil production.

5.4 Summary

Table 5.3 gives summary of important parameters of the under studied oil-wet cores.

Table 5.3 Summary of results, water-wet core samples

Parameter	Bentheim water-wet	Berea water-wet
Diameter, [cm]	3.79	3.76
Length, [cm]	24.3	24.95
Pore volume, [cm^3]	58.62	63.51
Porosity, [%]	21.34	22.83
Permeability, [md]	2314	842
$S_{wi,}$ [%]	22.82	35.06
$S_{or,}$ [%]	39.92	36.37
Core sample weight, [g]	567.81	388.97
Retention, [μg/g]	15.7	61.65
IPV, [%]	7.5	14.9
R_{rf}	1.39	8.56
BT time, [PV]	0.50	0.46
Rate of water flooding ml/min	0.2	0.9
Oil production at BT, [ml]	22.8	19.3
Final PV injected	4.2	27.9
Total oil production at final injected PV, [ml]	23.55	19.9

6 Polymer Flow in oil-wet core samples

6.1 Introduction

In this chaoter Berea and Bentheim cores which their wettability have been altered were studied and the results are presented. The wettability alterations have been evaluated and polymer behavior in porous media has been studied.

6.2 Bentheim oil-wet Core sample

6.2.1 Wettability

Core properties are mentioned in **Table 3.3**. Refer to section 3.3 (Core flooding Experiments) SSW was used to flood the core at constant rate of 0.9 ml/min in order to measure S_{or} and the pressure difference across the core and amount of oil production was recorded as a function of time. Pressure was build up rapidly before SSW breakthrough due to two phase flow inside the core as shown in **Figure 6.1**.

Breakthrough occurred after approximately 0.35 pore volume of injected SSW and after that, the pressure stabilized at approximately 200 mbar. **Figure 6.2** suggests that after breakthrough there is a decrease in pressure drop across the core which can be interpreted as oil production. **Figure 6.1** also verifies this interpretation by showing an increase in oil recovery after breakthrough.

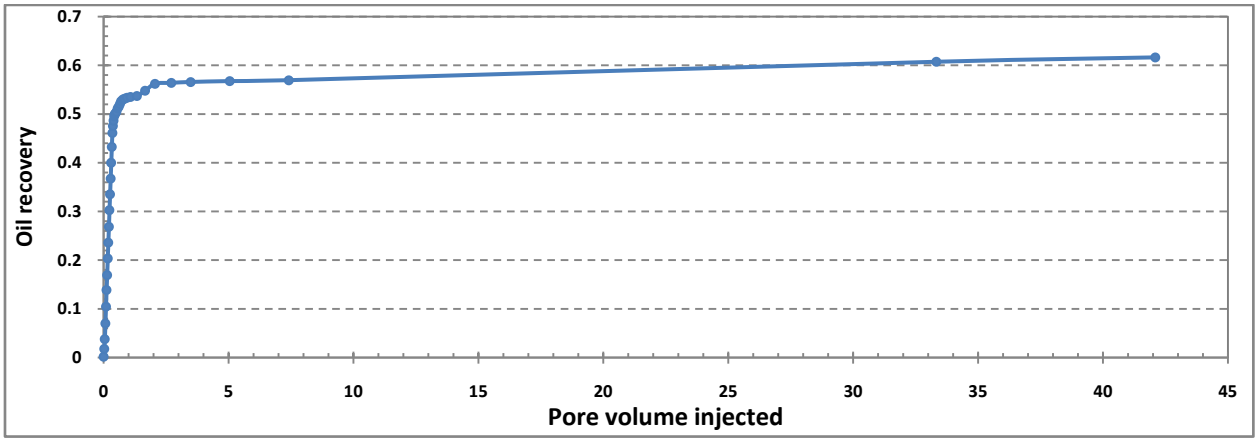

Figure 6.1 Pressure profile of SSW injection in 0.9 ml/min through Bentheim oil-wet

By close investigation of **Figure 6.1**, it can be observed that despite the production profile of typical water-wet core samples; here we do not have a smooth curve at breakthrough time. Instead, it seems that two breakthroughs have happened. One reason could be due the core being partially oil wet and partially water wet.

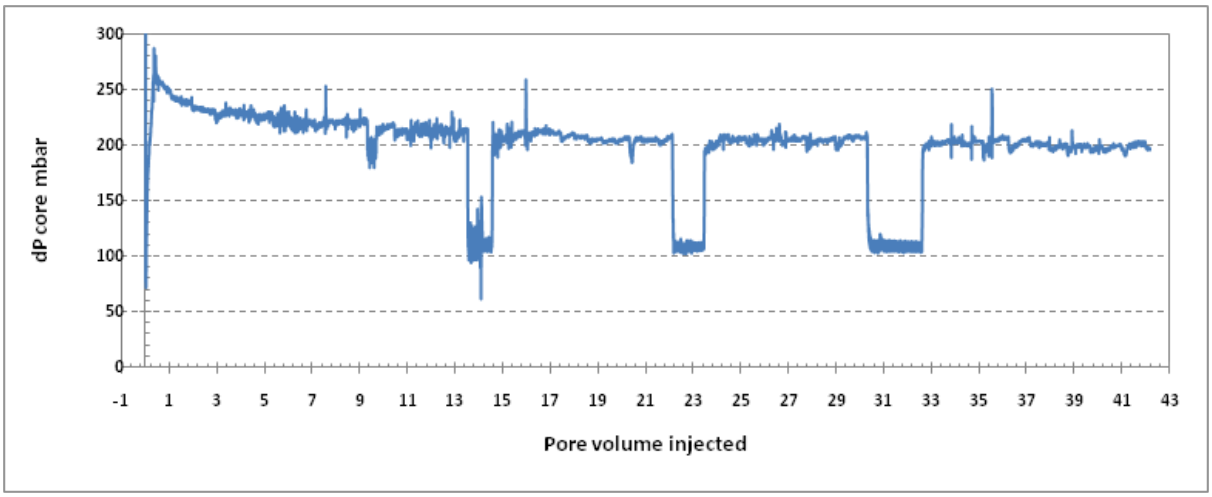

Figure 6.2 Pressure drop across the core during water flooding, Bentheim oil-wet

It is worth mentioning that the three lowest readings in **Figure 6.2** are because of malfunction of the pump.

6.2.2 Polymer behavior in porous media

After reaching to S_{or} following SSW flooding at a rate of 0.9 ml/min, the first polymer flooding at a constant rate of 0.2 ml/min was performed, followed by SSW flooding at the same rate. The second polymer flooding was started at the rate of 0.2 ml/min afterwards, flooding was continued until polymer breakthrough occurred and the difference pressure across the core stabilized, then the polymer flooding was gone on in different rates. The pressure drops across the core and capillary tube were recorded in one minute per sample.

From **Figure 6.3** abnormal fluctuations can be observed in capillary tube pressures. The color of effluent has been changes from colorless liquid to green and it became jelly-like colloid. It could be because of interaction between polymer and core treating fluid at presence of oil.

Polymer retention

Graphical illustration in **Figures 6.3** shows that polymer breakthrough happened when the capillary difference pressure reached to 14 mbar.

In **Figure 6.4** it is hard to indicate breakthrough time. Since in the previous case capillary tube pressure of breakthrough time was 14 mbar, in this case this value is considered as breakthrough time as well.

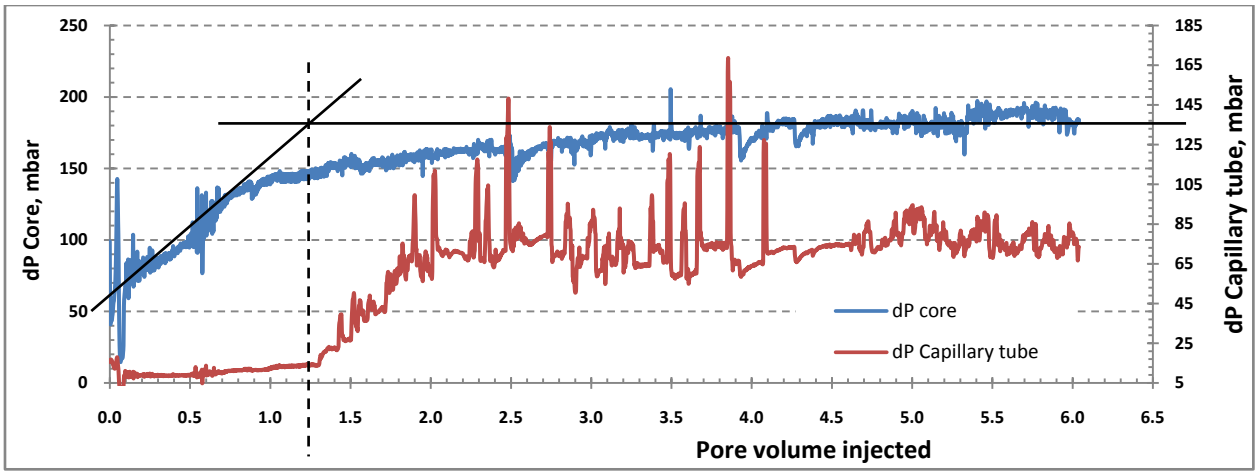

Figure 6.3 Polymer breakthrough in the first polymer flooding through Bentheim oil-wet core

Polymer breakthrough happened after injection of 1.126 and 0.66 pore volumes in the first and second polymer flooding, respectively (see **Figures 6.3** and **6.4**). Therefore 0.466 pore volume of polymer was retained inside the core. Given that the actual pore volume of the core is 38.51 cm^3, and core sample weight of 445.85 g, 16.1 micrograms of polymer per gram of the core was retained.

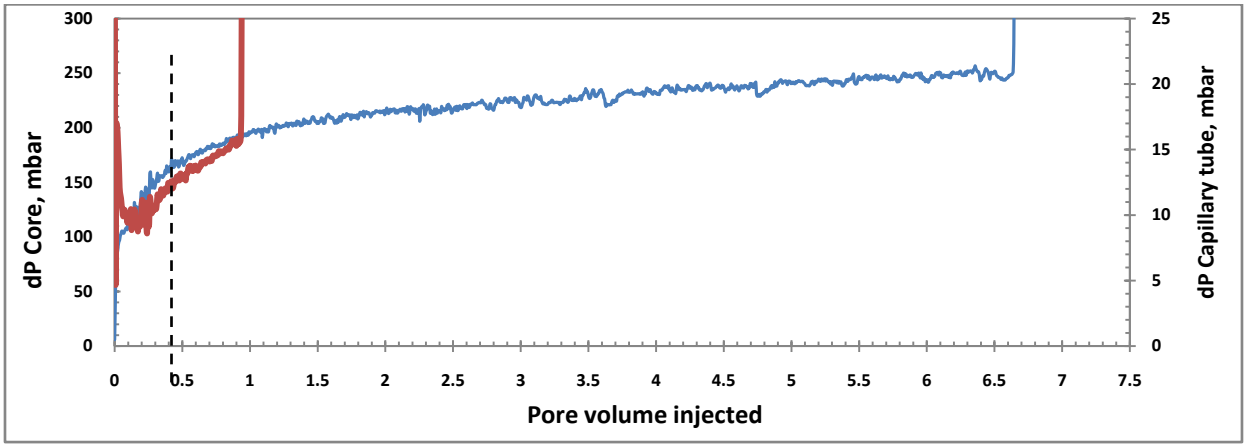

6.4 Polymer breakthrough in second polymer flooding through Bentheim water-wet core

Inaccessible pore volume, IPV

In order to determine the IPV, SSW flood was performed after the first polymer flooding and followed by a second polymer flooding both with rate of 0.2 ml/min.

The amount of pore volume where water flows through is (1-S_{or}) = 0.67. Since, in this study all saturation values are determined using fluid injection which flows through connected porous media and assuming piston like displacement, water breakthrough is actually after 0.67 pore volume of SSW injection. As it was mentioned, the polymer breakthrough after 0.66 pore volume injection. Therefore 1.8 percent of pore volume was inaccessible for polymer to flow through. This is very small and a possible reason could be because of high

permeability of core sample another explanation is the abnormal behavior of pressure in capillary tube which makes this reading unreliable. Therefore from now on this parameter is not included in the graphs.

Permeability reduction

Figures 6.2 and 6.5 show water flooding stabilized pressure difference across the core, before and after polymer flooding; there is approximately 100 mbar increase in the reading pressure after polymer flooding. By having pressure difference and core properties (**Table 3.3**) water effective permeability can be easily calculated which are 141.87 md and 57.02 md before and after polymer flooding respectively. This gives R_{rf} factor of R_{rf} = 2.48.

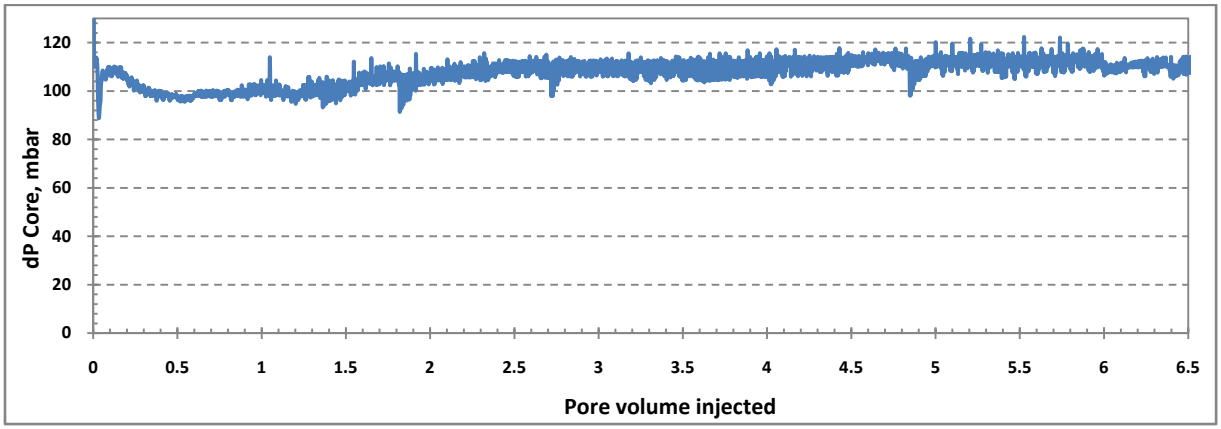

Figure 6.5 Water breakthrough in water flooding after first polymer flooding through Bentheim oil-wet core

6.2.3 Apparent viscosity and resistance factor

Apparent Viscosity

As a part of the second polymer flooding, a multi rate flooding was performed (**Figure 6.6**). Apparent viscosity and shear rate have been calculated using equations 5.1 and 5.2. Oil production, apparent viscosity and other parameters for second polymer flooding are shown in **Table 6.1**.

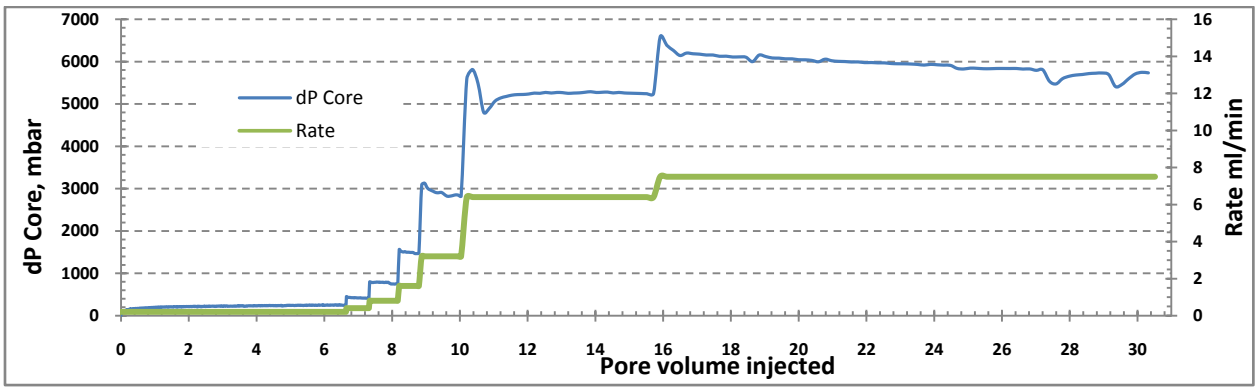

Figure 6.6 Multi rate Polymer flooding through Bentheim water-wet core

The permeability, k, which is used to calculate the apparent viscosity and shear rate was the effective permeability of SSW (57.02 md) after polymer flooding in order to reduce the effect of polymer retention on SSW permeability. This value was kept constant in calculating apparent viscosity and shear rate for all injection rates (**Figure 6.7)**.

Table 6.1 Apparent viscosity from Darcy law in second polymer flooding

Injection rate ml/min	dP core mbar	shear rate 1/s	Apparent viscosity mPa.s	oil Production ml
0.2	250	102.73	2.563084	0
0.4	411	205.46	2.106855	0
0.8	783	410.93	2.006895	0
1.6	1467	821.85	1.880022	0
3.2	2822	1643.70	1.808256	0
6.4	5241	3287.41	1.67914	0.4
7.5	5730	3852.43	1.566557	0

In **Figure 6.7** a decreasing trend can be detected. However, referring to section 5.2.3, this trend is not expected. This behavior can be justified by considering the observed green, jelly-like of the effluent and the abnormal pressure of capillary tube. Therefore the polymer does not have its original properties such as viscosity. Considering these points, calculated F_r does not have scientific value.

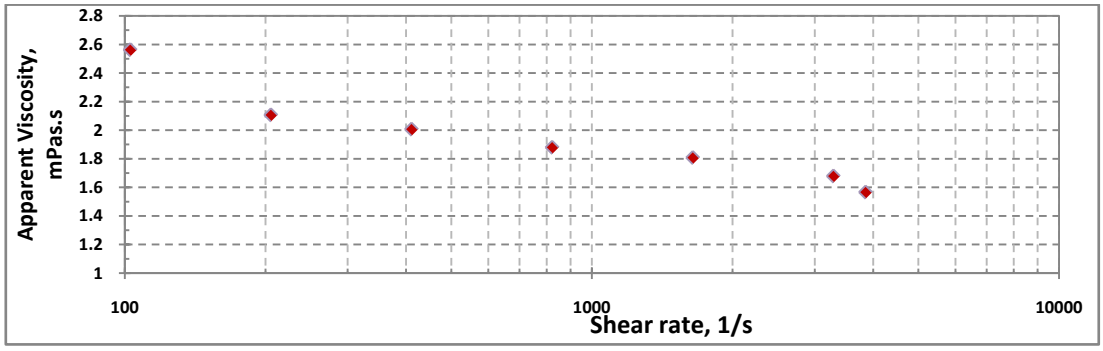

Figure 6.7 Darcy apparent viscosity, Bentheim oil-wet core

6.3 Berea oil-wet Core sample

6.3.1 Wettability

Berea is a water-wet sandstone rock however, in this work it has been treated to alter its wettability to oil wet. Wettability of the core was determined by interpretation of the oil production profile (refer to section 5.2.1. for more information).

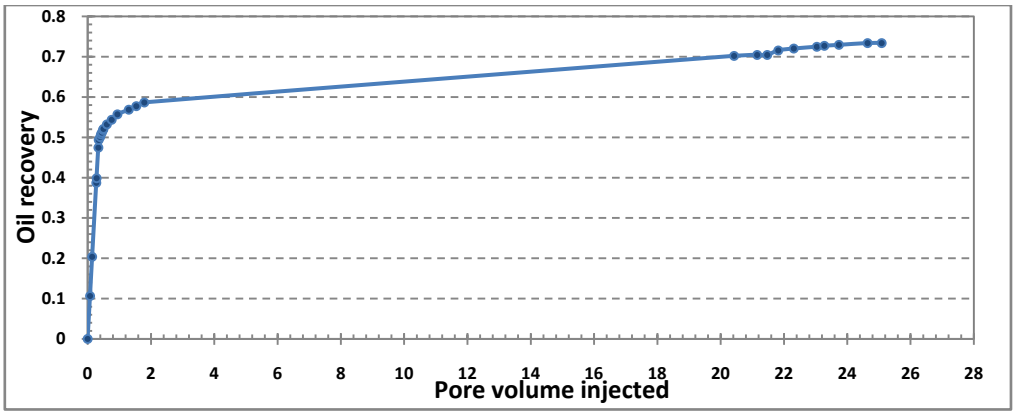

Figure 6.9 Oil recovery of SSW injection in 0.9 ml/min through Berea oil-wet core

Oil was displaced by SSW at constant rate of 0.9 ml/min with the mobility ratio of 1.88 and the pressure difference across the core and amount of oil production was recorded as a function of time. Pressure was build up rapidly before SSW breakthrough due to two phase flow inside the core as shown in **Figure 6.9**. Breakthrough happened after 0.35 pore volume injection of SSW then the pressure stabilized had a decreasing trend with small steepness at the late phase. The conclusion is there is oil production after breakthrough (**Figure 6.9** and **6.10**) which is the typical behavior of an oil-wet core. In the next step, the rate was increased to 2 ml/min, in order to avoid any oil production further in polymer flooding process.

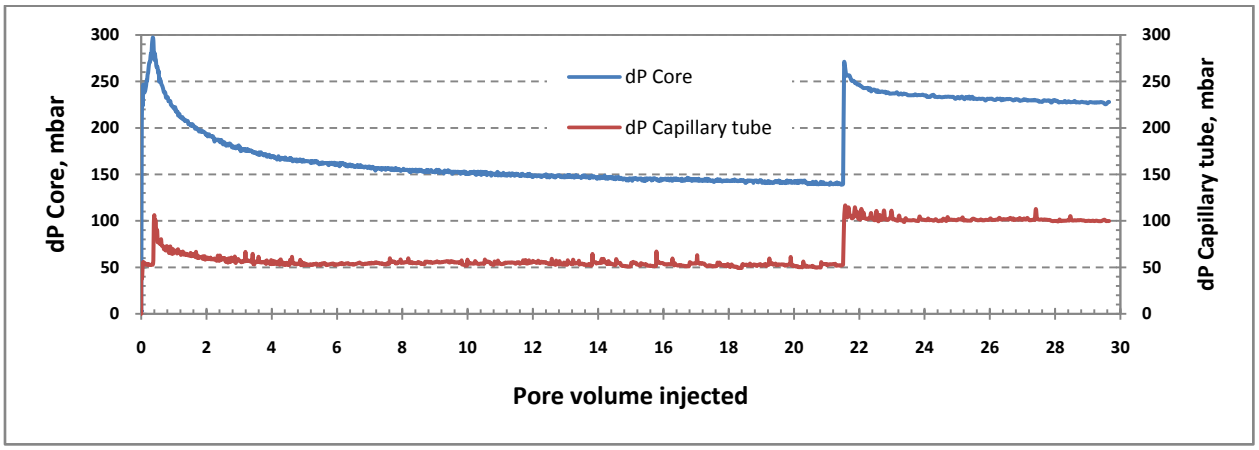

Figure 6.10 Pressure profile of SSW injection in 0.9 ml/min through Berea oil-wet

6.3.2 Polymer behavior in porous media

Polymer retention

The pressure differences across both core and capillary tube in the first and the second polymer floods are plotted in **Figures 6.11** and **6.12** with injection rate of 0.2 ml/min. It seems to be very difficult to determine the polymer breakthrough from the pressure drop across the core. Therefore pressure profile of capillary tube is used to determine the breakthrough

time. Breakthrough occurs when the capillary pressure is equal to the average value of pressure before and after breakthrough, about 14 mbar.

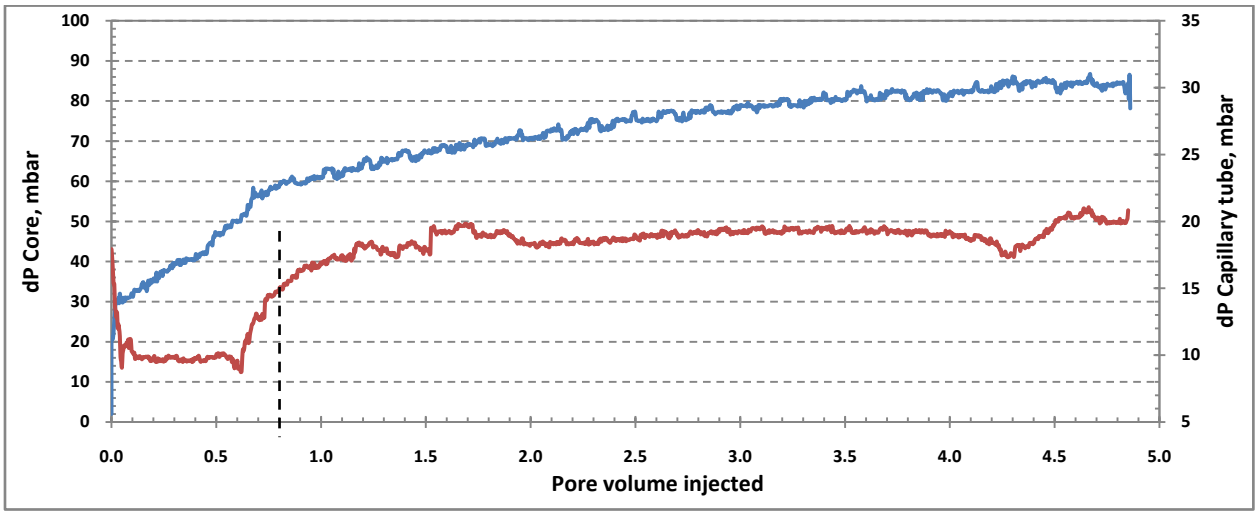

6.11 Polymer breakthrough in the first polymer flooding through Berea oil-wet core

Note that as stated in section 4.4, the average pressure is associated with the polymer solution with concentration of 50 percent to injecting solution concentration.

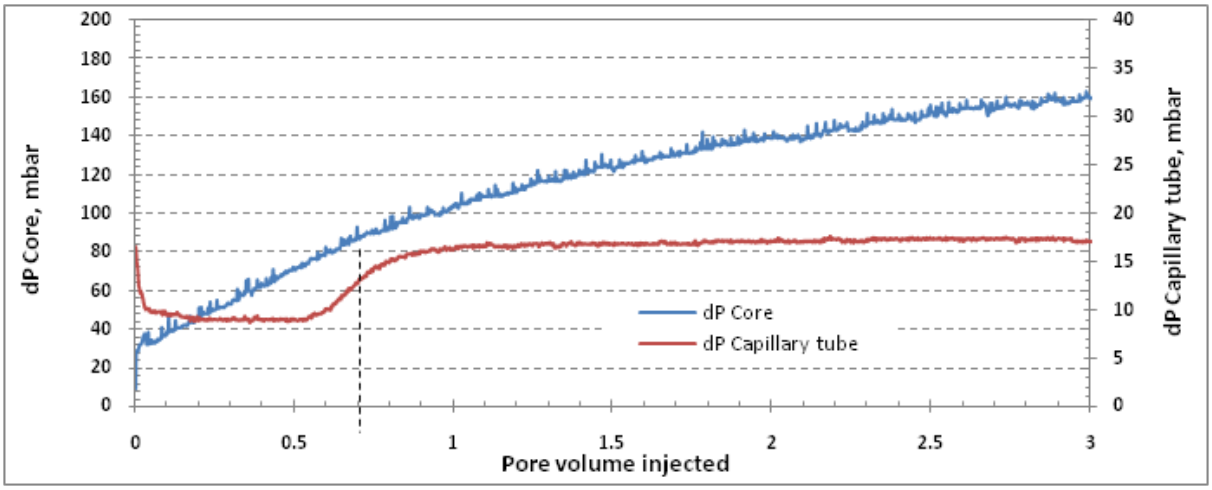

6.12 Polymer breakthrough in the second polymer flooding through Berea oil-wet core

Polymer breakthrough happened after injection 0.8 and 0.705 pore volumes for the first and second polymer floods, respectively. Therefore polymer solution of 0.095 pore volume was retained inside the core. Given that the pore volume of the core is 60.61 cm^3, and core sample weight 391.87 g, 5.84 micrograms of polymer per gram of the core was retained inside the core.The calculated retention is low possibly due to wettability alteration.

Inaccessible pore volume, IPV

The amount of pore volume available for the water to flow through is $(1-S_{or})$ = 0.777. This means that the water breakthrough occurs after 0.073 pore volumes of water injection (assuming piston-like displacement). Polymer breakthrough in the second polymer flooding

experiment happened after 0.705 pore volumes of polymer injection. Therefore the IPV value is 7.23 percent of pore volume. In contrary to the low retention value, the IPV is rather high.

Permeability reduction

To determine the permeability reduction of water, SSW was injected after first polymer flooding, **Figure 6.13**. From the Figure an increasing trend of pressure after breakthrough and some pressure fluctuation across the Capillary tube are visible. The pressure of core just after breakthrough was picked to calculate the water effective permeability. The effective permeability of water was decreased from 281.18 md to 232.08 md. Consequently the R_{rf} became 1.31.

6.13 Water breakthrough in water flooding after first polymer flooding through Berea oil-wet core

Multiple polymer flooding with various rates (0.2, 0.4, 0.8 and 0.03 ml/min) have been studied, see **Figure 6.14**. As it is depicted in the figure, the stabilized pressure has not been achieved in any rate and it was constantly increasing.

It was conceived that this increasing pressure could be the effect of oil relocation and accumulation at the end of core. Attempts have been made to flood the core by water with high rates (creating high viscous force) to push the oil out of the core (**Figure 6.15**).

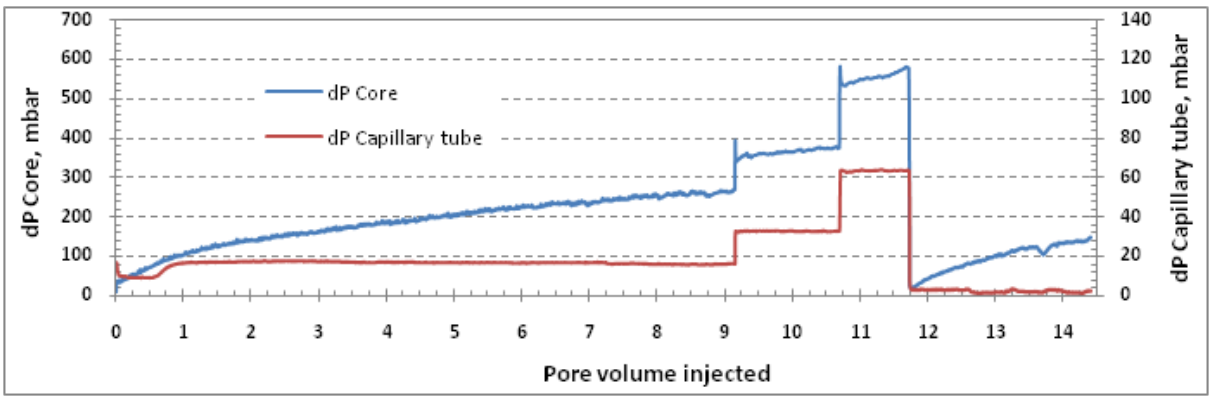

6.14 Multi rate Polymer flooding through Berea oil-wet core

The flooded rates were 0.2, 1, 3, 5, 7 and again 0.2 ml/min for comparing with the first flow rate. In rates 3, 5 and 7 ml/min oil production can be seen from the figure by first pressure decrease of dP core curve and secondly by observing small fluctuations in the capillary tube pressure. The amount of oil production was 2.1 ml after 32 pore volume injection which is a small value.

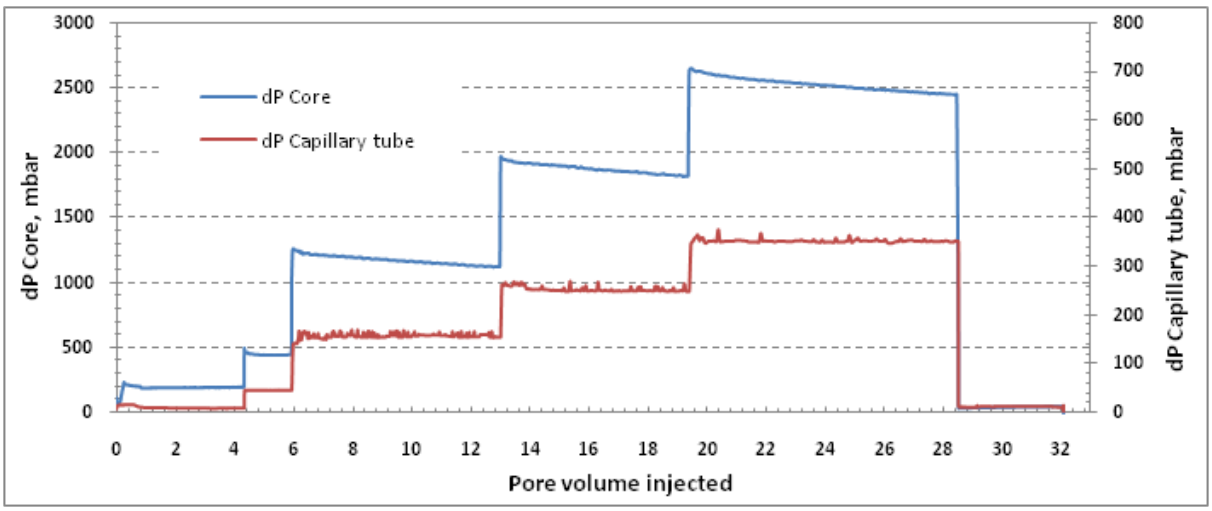

6.15 Multi rate water flooding through Berea oil-wet core

In the next step a new polymer flooding session has been started, **Figure 6.16**. From the figure increasing pressure of the core can be spotted and is a sign that the conceived reason is not valid. Therefore continuing of the process was canceled

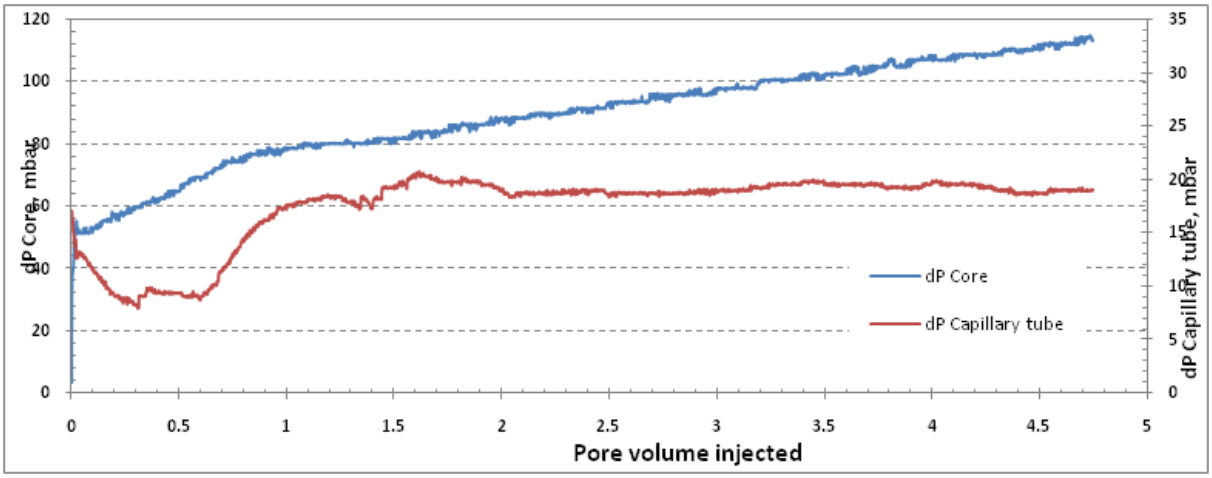

6.16 Third polymer flooding through Berea oil-wet core

6.4 Summary

Table 6.2 gives summary of important parameters of the under studied oil-wet cores.

Table 6.2 Oil-wet cores parameters

Parameter	Bentheim oil-wet	Berea oil-wet
Diameter, [cm]	3.79	3.77
Length, [cm]	18.6	24.96
Pore volume, [cm^3]	38.51	60.61
Porosity, [%]	18.33	21.27
Permeability, [md]	1007	758
S_{wi}, [%]	27.95	27.17
S_{or}, [%]	32.20	22.27
Core sample weight, [g]	445.85	391.87
Retention, [μg/g]	16.1	5.84
IPV, [%]	1.8	7.23
R_{rf}	2.48	1.31
BT time, [PV]	0.35	0.35
Rate of water flooding ml/min	0.9	0.9
Oil production at BT, [ml]	12.8	21.8
Final PV injected	42.1	21.5
Total oil production at final injected PV, [ml]	17.1	31.1

7 Discussion

Note: Most of the discussions have done in previous chapters with results. Here are comparisons of the results between different chapters.

Bulk viscosity, effect of salinity

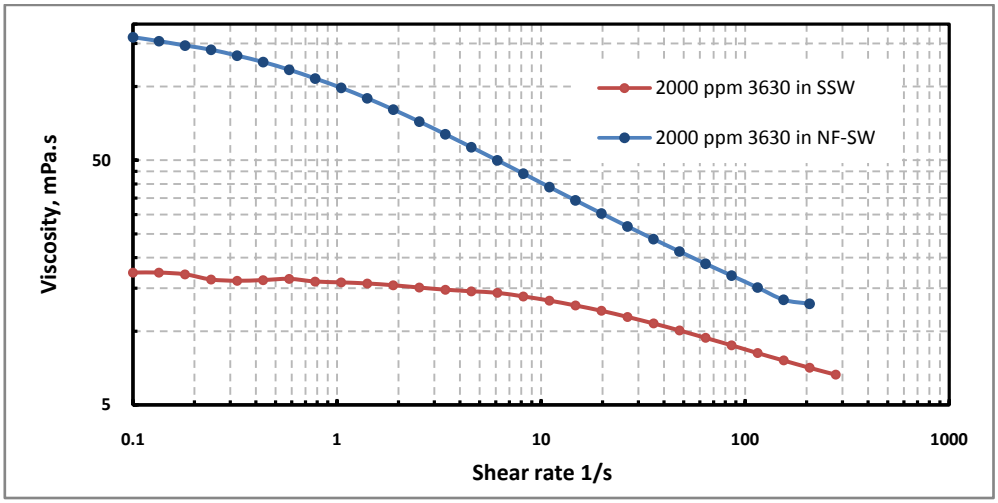

Figure 7.1 Effect of solvent salinity on viscosity of polymer 3630

Salinity decreases the viscosity of polymer solutions significantly especially synthetic one Such as Hydrolyzed polyacrylamide, HPAM. **Figure 7.1 and 7.2** give a comparison between 2000 ppm of both polymer 3630 and 3230 in SSW and NF-SW. Refer to Table 3.2 both salinity and divalent ion content of SSW is much higher than NF-SW. As the salinity of solution increases, the extension of polymer decreases and the solution viscosity declines.

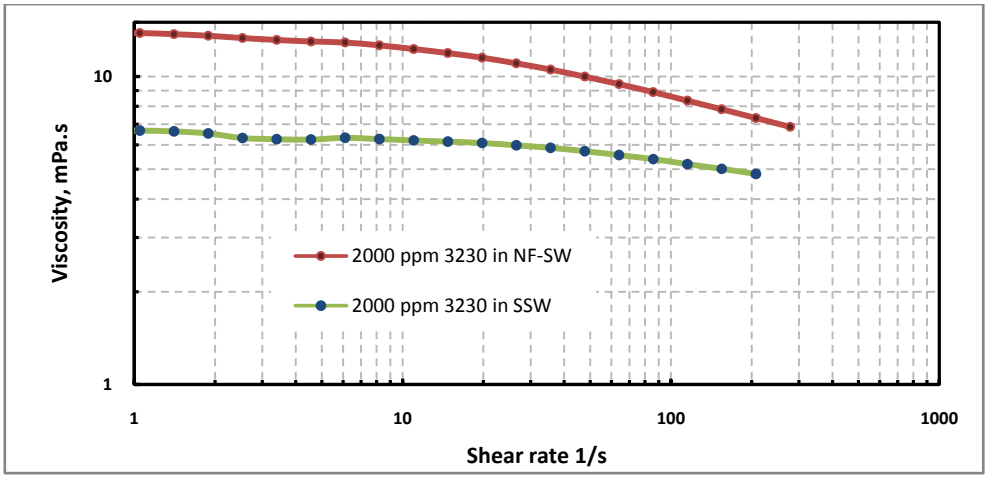

Figure 7.1 Effect of solvent salinity on viscosity of polymer 3630

Bulk viscosity, effect of Molecular weight

Molecular weight is one of the important factors which affect polymer viscosity. Refer to **Table 3.1**, the molecular weight of polymer 3630 is higher than 3230. **Figure 7.3** compares viscosities of these two polymers as a function of shear rate. For higher viscosities of the polymer the shear thinning regime starts at lower shear rates.

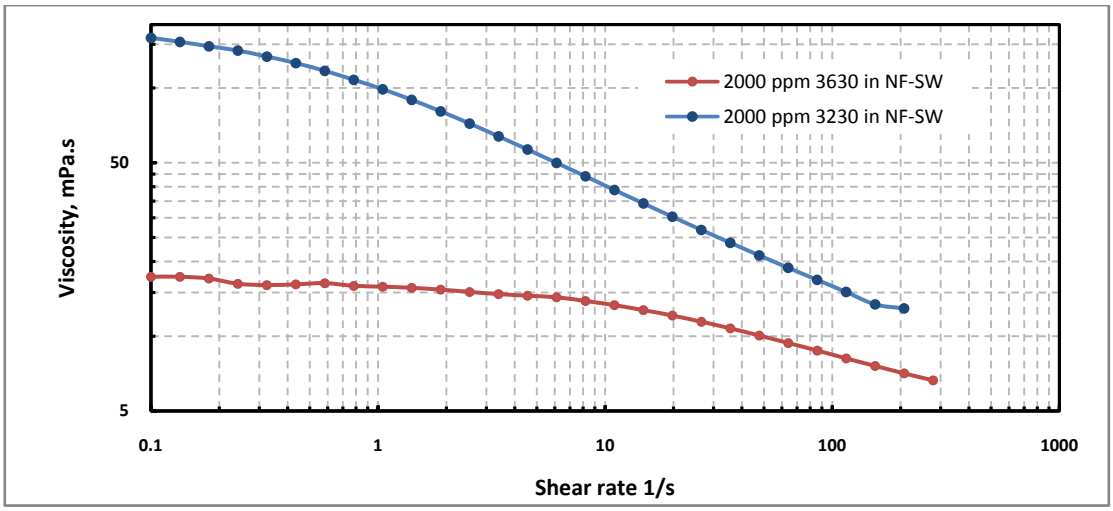

Figure 7.3 Effect of polymer molecular weight

Non-Newtonian fluid flow in capillary tube

For calculating viscosity of the injected polymer (400 ppm 3630 in SSW) intrinsic viscosity and Haggins constant have been utilized. Due to low concentration of the polymer and power law constant close to one, the equation 4.7 gives a very well mach with the observed pressure data from capillary tube. Therefore the new setup was effective because of having instantaneous measurements and possibility of putting the whole system under pressure and running the experiment.

Wettability alteration

Figures 7.4 ,7.5 , 7.6 and **7.7** show the normalized oil recovery against pore volume of water injection for Berea and Bentheim respectively. **Figures 7.5** and **7.7** show the first one porevolume injected of the normalized oil recovery against pore volume. In these figures the behavior of water wet cores can be easily seen. In the former the oil production after breakthrough is significant which can be indication of strongly oil-wet core. However in the latter the oil production is rather small and the transaction before and after breakthrough is not smooth, which can be interpreted as a intermediate oil wet.

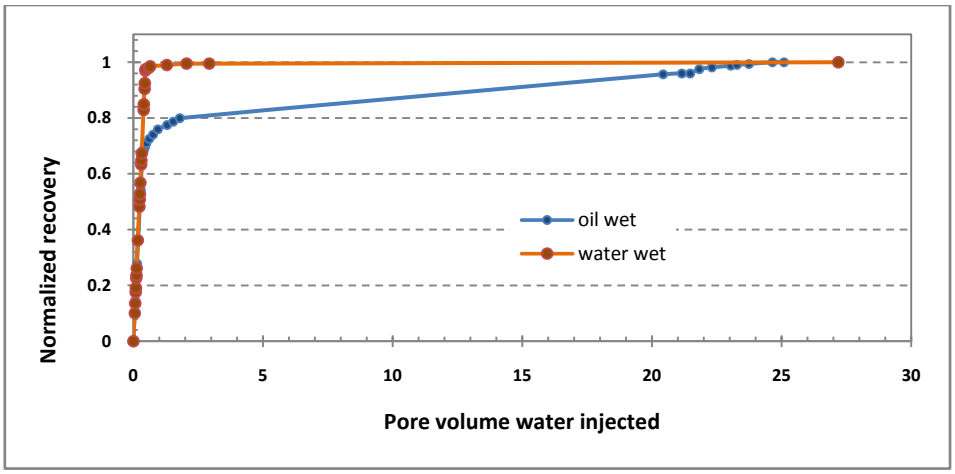

Figure 7.4 Normalized oil recovery, Berea cores

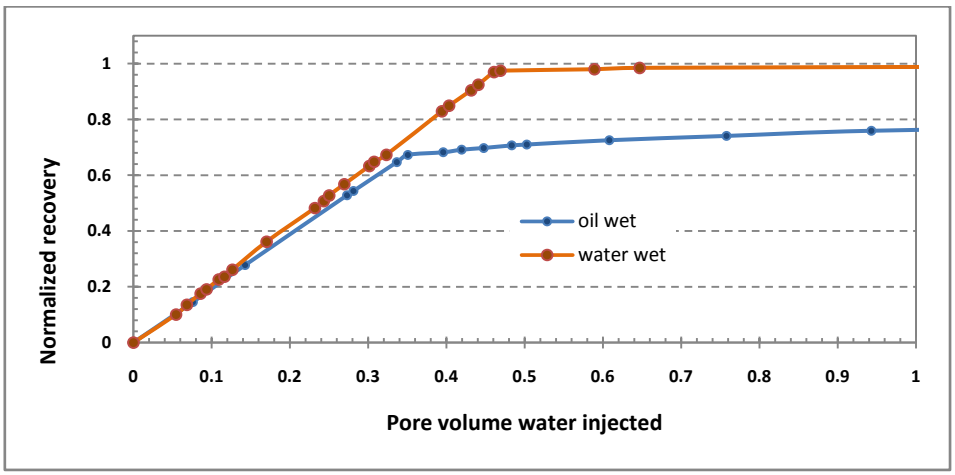

Figure 7.5 Normalized oil recovery, Berea cores (1st pore volume injected)

Another approach to determine the wettabillity is to look at the pressure profiles across the core (see section 5.2.1). The amount of pressure drop after breakthrough can be use as an indicator for estimating how oil-wet the core could be.

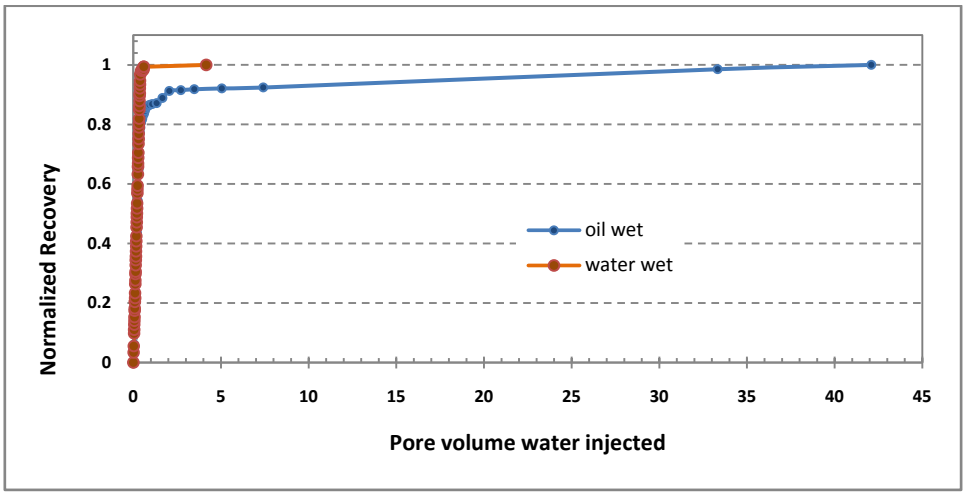

Figure 7.6 Normalized oil recovery, Bentheim cores

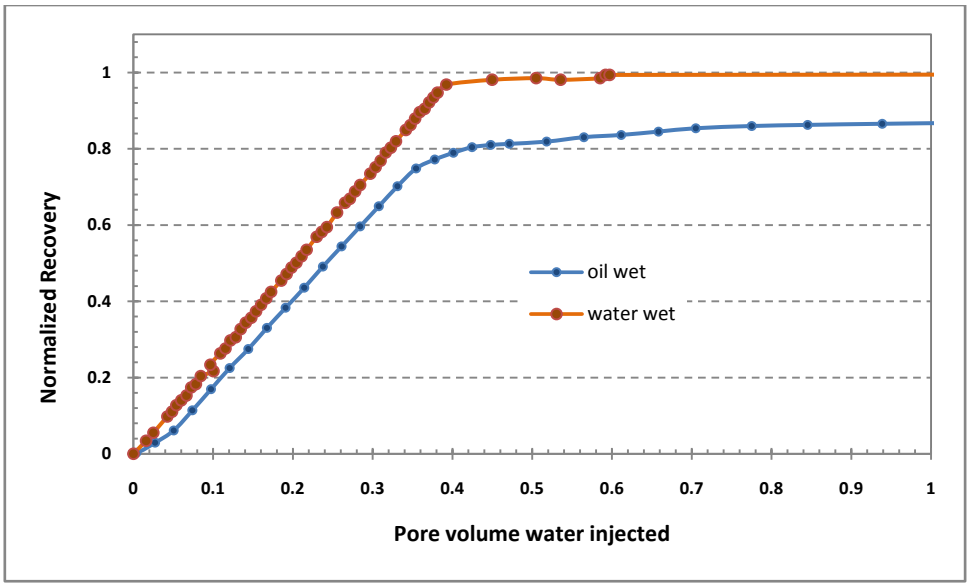

Figure 7.7 Normalized oil recovery, Bentheim cores (1st Pore volume injected)

Retention in water-wet cores

Figure 7.8 shows a breakthrough time in first polymer flooding for both Bentheim and Berea water-wet cores. It is important since all retention has occurred during this phase. As the figure suggests the amount of retention in Berea is much higher than Bentheim. Refer to **Table 5.3** IPV of Berea is also higher than Bentheim. They are due to lower permeability of Berea which leads to higher contact area interacting with polymer solution and smaller channel size and pore throat of Berea core sample. These make both adsorption and mechanical entrapment higher in Berae.

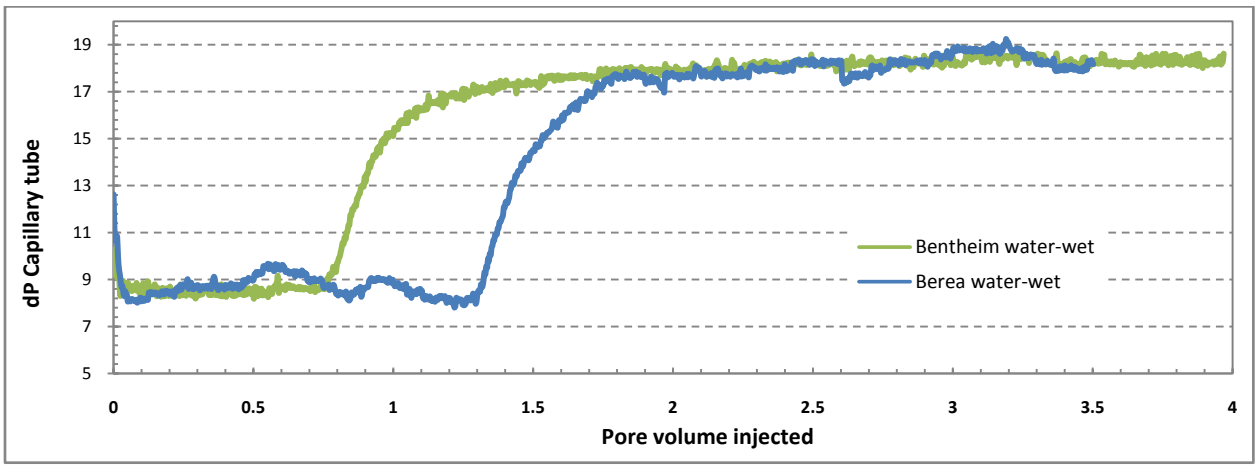

Figure 7.8 Breakthrough time in first polymer flooding for both Bentheim and Berea water-wet cores

Retention in Berea water-wet and oil-wet

Refer to **Table 6.2** and **Figure 7.9**, the retention value for Berea oil-wet is small and IPV is in acceptable range which suggests that the most of pore volume which associated to IPV have not been inaccessible by polymer entrapment. In the other words, there were already in accessible due to small pore size of pore throat. The reason that the surface adsorption in the Berea oil-wet is low could be due to the existence of an oil film which covers the inside surface of the core and reduces the contact area between the surface and polymer solved in the water.

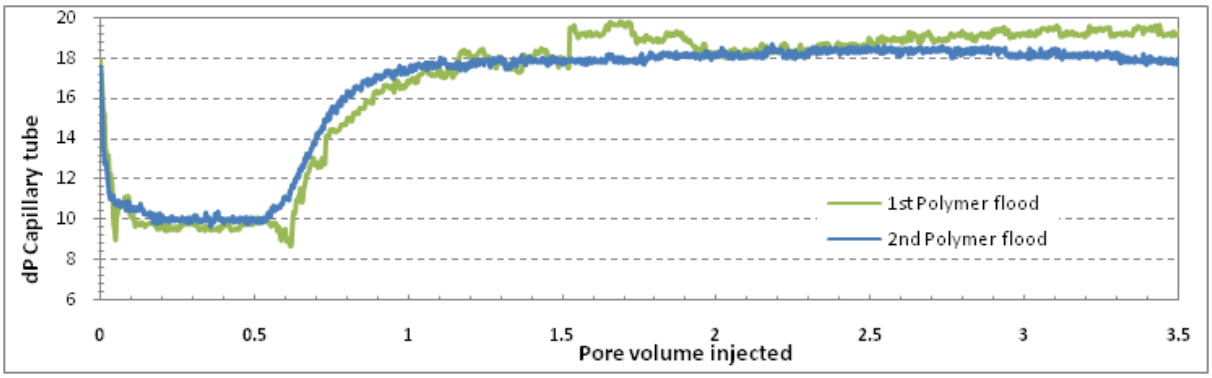

Figure 7.9 Breakthrough times in first and second polymer flooding for Berea oil-wet cores

Comparing IPV values for both Berea cores, there is more inaccessible pore volume for polymer in Berea water-wet core which is became inaccessible by polymer entrapment. Despite the fact that some amount of polymer which retained in porous media was trapped in channels, most of them were adsorbed on inside surface of the water-wet core.

Figure 7.10 shows the higher amount of retention in Berea water-wet than Berea oil-wet.

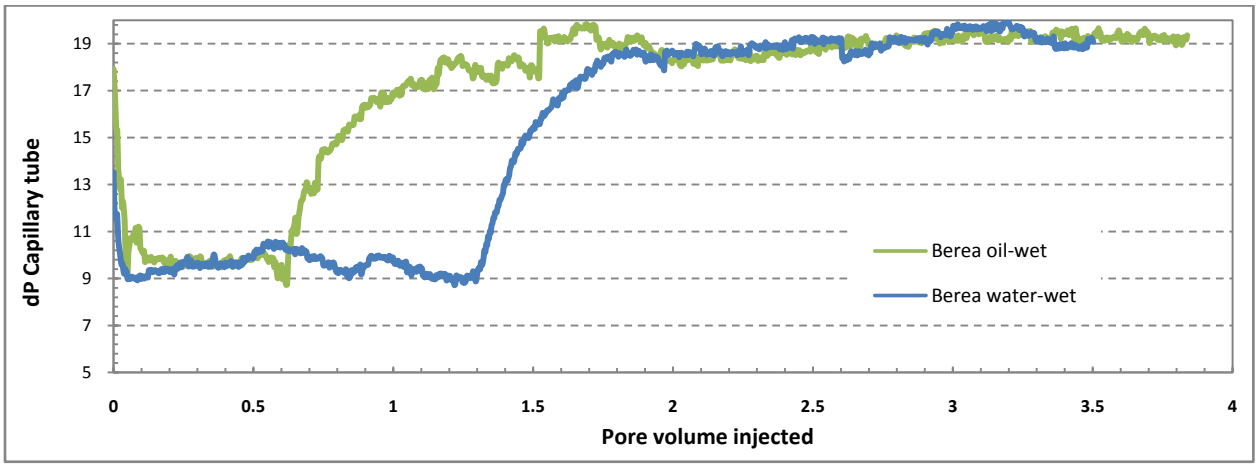

Figure 7.10 Breakthrough time in first polymer flooding for both Berea oil-wet and water-wet cores

Attempts have been made to do multiple rate polymer flooding on oil-wet cores but due change in polymer properties and not achieving stabilized pressure future work was impractical (Refer to section 6.2.3 and 6.3.2). However in water-wet cores the shear thickening and degradation regime were determined (see sections 5.2.3 and 5.3.3).

8 Conclusion and recommendation

The main conclusions of this work are summarized below.

- All polymer solutions showed both upper Newtonian and shear thinning flow regimes in our bulk rheology investigation. For each solution decreasing the polymer concentration resulted in a decrerased power law exponent, n, while the time constant, λ, increased. Also the effect of brine salinity on polymer viscosity was significant; for instance the viscosity of the 2000 ppm 3630 polymer in NF-SW was 153 mPa.s while in SSW was 15.6 mPa.s (approximately one tenth reduction). Moreover the effects of molecular weight was also high. For example the viscosity of 2000 ppm 3630 in NF-SW was 153 mPa.s while the viscosity of 2000 ppm 3230 in the same solution was only 13.1 mPa.s. Note that the polymer 3630 has a higher molecular weight than polymer 3230.
- The solution of 400 ppm 3630 polymer in SSW was used to conduct polymer flooding. Although the solution showed a shear thinning behavior, the power-law exponent was equal to 0.94.
- Calculated Huggins constants for all polymer solutions were in the range of a good solvent (0.4 ± 0.1). In addition, intrinsic viscosity value which indicates the size of polymer molecule in the solution was also affected by salinity and molecular weight. Solution with higher intrinsic viscosity is either in low salinity solvent or has high molecular weight.
- Polymer solution measurements were conducted on a capillary tube attached at the end of the core outlet during the core flood experiments. The shear thinning regime for polymer solution flow in capillary tube was observed at low flow rates (<1.5 ml/min). Since the power law exponent of the polymer solution was very close to one, shear rates were calculated using Newtonian fluids equation introducing a 1.6 percent error to the computed results.
- A model was developed to determine polymer concentration from pressure drop across the capillary tube. The viscosity of the polymer solution was derived as a function of polymer concentration at the shear rate of 130 s^{-1} (corresponding to injection rate of 0.2 ml/min) using the Huggins constant and the intrinsic viscosity for the 3630 polymer in SSW
- The wettability of all core samples was evaluated using both oil and water production measurements along with the pressure drop profiles recorded across the core. It appears that after the main water breakthrough a second smaller one occurred based on the oil production profile. The pressure and oil production profiles of water flooding for the Bentheim core indicated that rather a small volume of oil was produced after polymer breakthrough, and therefore the core can be considered as intermediate wet. The pressure and oil production profiles of water flooding for the Berea core showed oil

production after breakthrough which means the wettability-altered Berea core was oil-wet.

- The chemical treatment of the Bentheim core for wettability alteration proved to not be reliable, since greenish, jelly-like, treatment material was coming out and the recorded polymer flooding results were deemed non reliable and excluded from the analyses conducted for this core.
- Comparing the results of polymer flooding from Berea and Bentheim water-wet cores, the retention in the Berea formation was much higher than the Bentheim one. This is because of lower permeability and higher surface area in contact with polymer in the Berea as well as difference in rock surface composition and clay minerals. The IPV value of the Berea was higher than the Bentheim as well due to lower permeability and smaller pore throats in the Berea. High polymer retention and high IPV of the core lead to higher reduction of the permeability (R_{rf}) after the polymer flooding.
- In the oil-wet Berea formation the amount of retention is very low, which means wettability had a significant effect on this parameter. Apparently, oil covers the surface area of sand grains thus preventing polymer to have contact with the solid surface. Although the retention value was low, still 7.5 percent of core was inaccessible to polymer, which is due to low permeability of the core and the large size of polymer molecules.
- Comparing the Berea oil-wet and water-wet cores, the polymer retention is much lower in the oil-wet core. The IPV value in Berea water-wet is higher than the oil-wet one which shows that some extra pore volume of the Berea water-wet core has been blocked due to polymer entrapment.

Recommendations

The pressure drop across the core was very low so more accurate results can be obtained using a transmitter with low range of measurement and higher accuracy. The other way is to increase the length or reduce the diameter of the capillary tube (the latter increases the risk of tube blocking as well).

Since the retention in oil-wet Berea core is very low, any decrease in permeability is due to polymer entrapment. Therefore the core is very good candidate to study polymer entrapment mechanisms.

Appendix

Core treating Material

In order to alter the wettability of Berea and Bentheim core, Quilon has been used to treat the cores. Quilon is a solution chemically reactive complex in which a C_{14}-C_{18} fatty acid coordinated with traveling chromium. Seven grade are available : C, M, S, H, C-9 and L-11.

The procedure of treating is as follows:

- Saturate the core with Qualin 3% type L
- Flood the core with Qualin 3% from both side for several porevolumes
- Put the core in 90 ^{o}C for 7 to 9 days.

Bulk viscosity measurements

Table A.1 Measured viscosity using the polymer 3630 in SSW at 20˚C.

Shear rate 1/s	Viscosity, mPa.s						
	100 ppm	250 ppm	500 ppm	750 ppm	1000 ppm	1500 ppm	2000 ppm
499.9	1.966	2.235	2.647	3.112	3.721	4.719	6.144
372.7	1.739	1.999	2.427	2.934	3.583	4.736	6.321
277.9	1.567	1.838	2.286	2.847	3.555	4.874	6.644
207.2	1.459	1.75	2.23	2.854	3.63	5.115	7.088
154.4	1.381	1.697	2.22	2.904	3.748	5.394	7.593
115.1	1.33	1.674	2.237	2.969	3.882	5.693	8.143
85.84	1.324	1.695	2.283	3.067	4.048	6.027	8.76
63.99	1.309	1.704	2.318	3.149	4.201	6.352	9.393
47.71	1.314	1.735	2.36	3.242	4.366	6.692	10.07
35.56	1.32	1.767	2.405	3.331	4.528	7.03	10.76
26.51	1.315	1.784	2.434	3.396	4.666	7.34	11.44
19.77	1.327	1.807	2.471	3.469	4.806	7.64	12.12
14.74	1.314	1.825	2.487	3.51	4.903	7.881	12.74
10.99	1.33	1.985	2.499	3.55	4.994	8.107	13.34
8.19	1.341	1.933	2.563	3.599	5.091	8.294	13.87
6.105	1.355	2.248	2.557	3.634	5.15	8.456	14.35
4.552	1.302	2.18	2.53	3.584	5.094	8.464	14.56
3.393	1.274	2.067	2.563	3.604	5.136	8.487	14.78
2.53	1.342	2.271	2.635	3.651	5.23	8.64	15.08
1.886	1.57	2.835	2.788	3.834	5.402	8.778	15.41
1.406	1.712	3.45	2.897	3.959	5.501	8.91	15.67
1.048	1.666	3.955	2.877	4.021	5.517	9.067	15.83
0.7814	1.537	4.743	2.768	4.041	5.612	9.142	15.96
0.5825	1.594	5.874	2.891	4.121	5.586	9.325	16.36
0.4343	1.605	6.236	3.061	3.854	5.311	9.187	16.18
0.3238	1.484	8.183	3.422	3.523	5.89	8.869	16.07
0.2413	1.806	10.03	3.018	3.589	5.831	8.955	16.27
0.1799	1.635	13.15	3.188	3.569	5.817	9.587	17.08
0.1341	2.463	16.16	3.789	4.204	5.887	9.568	17.36
0.1	1.888	19.51	3.695	3.926	5.583	9.414	17.36

Table A.2 Measured viscosity using the polymer 3630 in NF at 20°C.

Shear rate 1/s	Viscosity, mPa.s						
	100 ppm	250 ppm	500 ppm	750 ppm	1000 ppm	1500 ppm	2000 ppm
499.9	2.379	3.324	4.665	5.749	7.229	9.899	12.89
372.7	2.119	2.991	4.287	5.306	7.182	10.26	13.83
277.9	1.876	2.613	3.843	4.983	6.685	10.38	13.91
207.2	1.707	2.386	3.634	4.744	6.131	9.103	12.95
154.4	1.61	2.338	3.639	4.998	6.51	9.836	13.45
115.1	1.547	2.331	3.774	5.293	7.021	10.84	15.09
85.84	1.541	2.379	3.953	5.637	7.583	11.95	16.88
63.99	1.536	2.424	4.129	5.986	8.167	13.15	18.88
47.71	1.554	2.497	4.333	6.382	8.816	14.51	21.18
35.56	1.58	2.578	4.556	6.817	9.535	16.04	23.81
26.51	1.595	2.648	4.785	7.278	10.32	17.76	26.83
19.77	1.629	2.746	5.046	7.799	11.2	19.72	30.31
14.74	1.639	2.82	5.296	8.326	12.15	21.91	34.29
10.99	1.672	2.915	5.575	8.904	13.18	24.36	38.84
8.19	1.712	3.024	5.871	9.514	14.3	27.13	44.1
6.105	1.76	3.142	6.171	10.14	15.45	30.1	49.95
4.552	1.702	3.127	6.326	10.61	16.55	33.29	56.54
3.393	1.678	3.153	6.563	11.13	17.72	36.7	63.86
2.53	1.755	3.286	6.874	11.76	18.94	40.35	71.93
1.886	1.964	3.51	7.168	12.37	20.1	44.06	80.55
1.406	2.077	3.705	7.464	12.95	21.19	47.75	89.59
1.048	2.174	3.844	7.609	13.21	22.03	51.19	98.86
0.7813	2.154	3.903	7.714	13.43	22.56	54.13	107.9
0.5825	2.391	4.132	8.102	13.93	23.3	57.1	117.2
0.4343	2.053	3.776	8.143	14.48	24	59.96	126
0.3238	2.271	3.683	8.203	14.18	24.21	62.06	133.8
0.2413	2.256	4.292	8.271	13.52	24.3	63.41	141.5
0.1799	2.678	4.385	8.147	13.67	24.06	64.15	147.2
0.1342	2.941	5.435	8.746	14.72	24.92	65.8	153.4
0.1	2.953	5.043	8.393	15.55	25.18	67.23	159.2

Figure A.3 Measured and matched viscosity versus shear rate, 3230S in SSW

Shear rate 1/s	Viscosity, mPa.s						
	100 ppm	250 ppm	500 ppm	750 ppm	1000 ppm	1500 ppm	2000 ppm
499.9	1.944	2.103	2.342	2.654	2.972	3.713	4.566
372.7	1.713	1.873	2.125	2.45	2.79	3.603	4.563
277.9	1.532	1.699	1.97	2.317	2.688	3.589	4.657
207.2	1.415	1.59	1.888	2.264	2.673	3.662	4.828
154.4	1.327	1.513	1.84	2.251	2.695	3.759	5.014
115.1	1.265	1.464	1.818	2.255	2.727	3.855	5.195
85.84	1.249	1.459	1.832	2.29	2.783	3.968	5.393
63.99	1.228	1.445	1.832	2.306	2.818	4.055	5.558
47.71	1.225	1.448	1.844	2.33	2.86	4.144	5.723
35.56	1.228	1.454	1.857	2.355	2.898	4.223	5.868
26.51	1.219	1.448	1.857	2.364	2.917	4.275	5.98
19.77	1.229	1.46	1.872	2.388	2.948	4.334	6.086
14.74	1.209	1.447	1.863	2.387	2.949	4.354	6.146
10.99	1.216	1.444	1.871	2.378	2.958	4.379	6.203
8.19	1.241	1.481	1.897	2.434	2.992	4.428	6.266
6.105	1.279	1.49	1.895	2.412	3.003	4.442	6.325
4.552	1.116	1.396	1.826	2.349	2.933	4.365	6.242
3.393	1.173	1.442	1.871	2.393	2.946	4.378	6.26
2.53	1.251	1.505	1.908	2.461	3.03	4.456	6.315
1.886	1.485	1.689	2.057	2.655	3.212	4.678	6.536
1.406	1.714	1.702	2.161	2.624	3.304	4.842	6.638
1.048	1.713	1.716	2.088	2.633	3.139	4.751	6.677
0.7813	1.839	1.787	2.135	2.576	3.182	4.654	6.694
0.5824	2.001	2.036	2.078	2.443	3.117	4.732	7.111
0.4343	1.289	1.613	1.897	2.65	3.295	4.861	6.654
0.3238	1.617	1.581	2.381	2.984	3.236	5.08	6.596
0.2413	2.305	2.163	2.256	2.12	3.26	4.669	6.998
0.1798	2.808	2.522	2.372	1.719	3.125	4.577	7.732
0.1341	2.177	2.703	1.905	1.9	4.538	5.112	8.206
0.1	2.285	1.765	2.055	1.592	4.027	5.141	7.277

Figure A.4 Measured and matched viscosity versus shear rate, 3230S in NF

Shear rate 1/s	Viscosity, mPa.s						
	100 ppm	250 ppm	500 ppm	750 ppm	1000 ppm	1500 ppm	2000 ppm
499.9	1.937	2.181	2.664	3.118	3.649	4.816	6.191
372.7	1.713	1.963	2.471	2.97	3.563	4.9	6.48
277.9	1.539	1.806	2.351	2.905	3.571	5.084	6.867
207.2	1.429	1.72	2.314	2.928	3.667	5.349	7.335
154.4	1.347	1.667	2.32	2.989	3.793	5.637	7.834
115.1	1.292	1.643	2.343	3.06	3.925	5.93	8.352
85.84	1.282	1.659	2.4	3.16	4.081	6.25	8.907
63.99	1.266	1.662	2.437	3.239	4.217	6.546	9.45
47.71	1.267	1.68	2.485	3.326	4.36	6.847	9.998
35.56	1.272	1.701	2.532	3.409	4.492	7.139	10.54
26.51	1.266	1.71	2.559	3.471	4.602	7.394	11.04
19.77	1.278	1.735	2.603	3.544	4.713	7.638	11.52
14.74	1.262	1.739	2.614	3.579	4.785	7.826	11.92
10.99	1.267	1.747	2.628	3.601	4.848	8.005	12.29
8.19	1.302	1.803	2.68	3.679	4.931	8.158	12.63
6.105	1.314	1.815	2.696	3.688	4.969	8.297	12.9
4.552	1.235	1.787	2.626	3.631	4.926	8.275	13
3.393	1.238	1.829	2.626	3.679	4.972	8.334	13.15
2.53	1.306	1.93	2.726	3.807	5.038	8.44	13.34
1.886	1.48	2.099	2.867	3.91	5.165	8.645	13.57
1.406	1.571	2.226	2.999	3.969	5.261	8.771	13.73
1.048	1.483	2.385	3.005	3.954	5.27	8.876	13.85
0.7814	1.543	2.569	2.902	3.879	5.297	8.948	13.87
0.5825	1.872	2.601	2.943	4.011	5.193	8.893	14.22
0.4343	1.585	2.495	2.871	3.905	5.328	8.977	13.8
0.3238	1.591	2.707	2.932	3.317	5.432	9.217	14.1
0.2413	1.775	2.908	2.799	3.441	4.846	8.703	13.72
0.1799	1.455	4.005	3.094	3.305	5.144	9.198	13.91
0.1341	2.84	4.786	3.114	4.696	4.951	9.018	13.49
0.1	2.83	4.88	2.817	4.062	5.603	9.673	14.26

References

Chauvetea, G and Zaitoun, A 1981. Basic Rheological Behaviour of Xanthan Polysaccharide Solutions in porous media: Effect of pore size and Polymer Concentration. In *Development of Petroleum Sience, 13 Enhanced Oil Recovery*, ed. F.J. Fayers. Amesterdam, Elsevier Scientific Publication Company.

Dawson, Rapier, Lantz, Ronald, B. Esso Production Research, Co. 1972. Inaccessible Pore Volume in Polymer Flooding. *SPE Journal, Volume 12, Number 5.*: 448-452, SPE 3522-PA

Don W. Green and G Paul Willhite. 1998. *Enhanced Oil Recovery*. Richardson, TX USA: SPE

Littmann W. 1988. *Polymer Flooding.* Amesterdam, Netherlands: Elsevier Science Publisher B.V.

Necmettin, M. 1969. Rheology and Adsorption of Aqueous Polymer Solutions. *Journal of Canadian Petroleum Technology*, *Volume 8, Number 2, 45-50.*

Sorbie, K.S. 1991. *Polymer-Improved Oil Recovery.* Glasgow, Scotland: Blackie and Sons Ltd.

Stavland, A. Jonsbraten, H. C. Lohne, A. Moen, A. And Giske, N.H., 2010. Polymer Flooding - Flow Properties in Porous Media Versus Rheological Parameters. Paper SPE presented at the SPE EUROPEC/EAGE Annual Conference and Exibition held in Barcelona, Spain, 14 – 17 June 2010. SPE 131103